# Early Neogene history of the Central American arc from Bocas del Toro, western Panama

**Anthony G. Coates**[†]
*Smithsonian Tropical Research Institute, P.O. Box 2072, Balboa, Republic of Panama*

**Marie-Pierre Aubry**[‡]
*Institut des Sciences de l'Evolution, Université de Montpellier, Montpellier, Cedex 5, France*

**William A. Berggren**
*Department of Geology and Geophysics, Woods Hole Oceanographic Institution, Woods Hole, Massachusetts 02543, USA*

**Laurel S. Collins**
*Department of Earth Sciences, Florida International University, Miami, Florida 33199, USA*

**Michael Kunk**
*U.S. Geological Survey, M.S. 963, Denver Federal Center, Denver, Colorado 80225, USA*

## ABSTRACT

**A newly discovered sequence of lower to middle Miocene rocks from the eastern Bocas del Toro archipelago, western Panama, reveals the timing and environment of the earliest stages in the rise of the Isthmus of Panama in this region. Two new formations, the Punta Alegre Formation (lower Miocene, Aquitanian to Burdigalian) and the Valiente Formation (middle Miocene, Langhian to Serravallian), are here named and formally described. The Punta Alegre Formation contains a diagnostic microfauna of benthic and planktic foraminifera and calcareous nannofossils that indicate deposition in a 2000-m-deep pre-isthmian neotropical ocean from as old as 21.5–18.3 Ma. Its lithology varies from silty mudstone to muddy foraminiferal ooze with rare thin microturbidite layers near the top. The Valiente Formation, which ranges in age from 16.4 to ca. 12.0 Ma, lies with slight angular unconformity on the Punta Alegre Formation and consists of five lithofacies: (1) columnar basalt and flow breccia, (2) pyroclastic deposits, (3) coarse-grained volcaniclastic deposits, (4) coral-reef limestone with diverse large coral colonies, and (5) marine debris-flow deposits and microturbidites. These lithofacies are interpreted to indicate that after ca. 16 Ma a volcanic arc developed in the region of Bocas del Toro and that by ca. 12 Ma an extensively emergent archipelago of volcanic islands had formed. $^{39}Ar/^{40}Ar$ dating of basalt flows associated with the fossiliferous sedimentary rocks in the upper part of the Valiente Formation strongly confirms the ages derived from planktic foraminifera and nannofossils. Paleobathymetric analysis of the two new formations in the Valiente Peninsula and Popa Island, in the Bocas del Toro archipelago, shows a general shallowing from lower- through upper-bathyal to upper-neritic and emergent laharic and fluviatile deposits from ca. 19 to 12 Ma. The overlying nonconformable Bocas del Toro Group contains a lower transgressive sequence ranging from basal nearshore sandstone to upper-bathyal mudstone (ca. 8.1–5.3 Ma) and an upper regressive sequence (5.3–3.5 Ma). A similar paleobathymetric pattern is observed from the Gatun to Chagres Formations (12–6 Ma) in the Panama Canal Basin area and in the Uscari, Rio Banana, Quebrada Chocolate, and Moin Formations (8–1.7 Ma) in the southern Limón Basin of Costa Rica.**

**Keywords: Neogene, Central America, Panama, Bocas del Toro, paleobathymetry, stratigraphy.**

## INTRODUCTION

The closure of the Isthmus of Panama triggered profound environmental, evolutionary, and ecological changes both on land and in the sea. The formation of a bridge between the North and South American continents gave rise to the great American biotic interchange on land (Webb and Rancy, 1996; Webb, 1999; Stehli and Webb, 1985). Less well known are the timing and nature of the changes in the sea consequent upon the rise of a sill or barrier between the eastern Pacific and the Caribbean. This marine barrier gradually affected ocean circulation during Neogene time. In the process, a striking contrast evolved between the relatively warm, more saline, nutrient-poor Caribbean and the more seasonal, less saline, and more productive (for pelagic organisms) eastern Pacific. These environmental changes apparently altered the course of evolution, first of the deep-water planktic organisms like radiolaria and diatoms from ca. 15 Ma, and then successively shallower taxa until complete emergence at ca. 4–3 Ma. The Caribbean became dominated by carbonate-associated benthic foraminifera and coral-reef–seagrass–mangrove coastal ecosystems and a profound taxonomic turnover occurred in corals and mollusks (Budd and Johnson, 1997; Jackson et al., 1993). In contrast, the Pacific has rich pelagic fisheries but poorly developed coral reefs (Jackson and D'Croz, 1999). The ability to demonstrate a causal relationship between

[†]E-mail: coatesj@hardynet.com.
[‡]Present address: Department of Geological Sciences, Rutgers University, Piscataway, New Jersey 08854, USA.

*GSA Bulletin*; March 2003; v. 115; no. 3; p. 271–287; 7 figures; 3 tables.

**Figure 1. Geologic map and cross section (a–a′; F—fault) of the Valiente Peninsula, Bocas del Toro, western Panama, showing the distribution of the Punta Alegre and Valiente Formations. The five lithofacies of the Valiente Formation are indicated by separate colors and numbers on the key (upper right) as follows: v1—basalt-lava and flow-breccia facies, v2—coarse-grained volcaniclastic facies, v3—pyroclastic facies, v4—coral-reef facies, and v5—marine debris-flow and turbidite facies. See text for descriptions of each facies. Numbers on the map locate the sites of samples used for this study (slashes are used to indicate site-number ranges). Details of sites may be obtained in the PPP Database at http://www.fiu.edu/~collinsl/. Vent centers were located at Llorona Hill and ~2 km east of Avispa Point. The extensive areas to the east of these centers mapped in red (v1 facies) are dominated by flow breccia with minor columnar basalt. The coarse-grained volcaniclastic fluviatile, estuarine, and shallow-marine facies (v2) always surrounds the v1 facies except along the northern margin of Bluefield Bay, where a pyroclastic facies (v3) is developed. Small coral-reef lenses (v4) are associated with the v2 facies, especially near Toro Point. A debris-flow and turbidite facies (v5) is developed along the northern coast around Cusapin Point.**

the environmental and biological changes rests largely on the availability of land-based isthmian sections bracketing the time involved and the establishment of a precise correlation within and between them.

In earlier papers, we established precise correlations for the late Neogene events in the southern Limón Basin of Costa Rica (Collins et al., 1995; McNeill et al., 1999), the Panama Canal Basin (Collins et al., 1996), and the Bocas del Toro Basin, Panama (Coates, 1999); here we describe an extensive, newly discovered sequence of lower to upper Miocene rocks from the Valiente Peninsula and Popa Island in the Bocas del Toro archipelago, western Panama (Figs. 1, 2) that provides the first complete record for this region of the nearshore history of the early stages of the rise of the Central American isthmus. The sequence provides a link between the lower Neogene section previously described in the southern Limón Basin of Costa Rica (Cassell and Sen Gupta, 1989a, 1989b; Bottazzi et al., 1994) to the northwest and the Panama Canal Basin to the southeast. These sections reveal different local geologic histories and thus the necessity of closely spaced data points if the paleogeography of the rise of the southern Central American isthmus is to be accurately reconstructed.

The Bocas del Toro sequence reveals four phases in the rise of the isthmus: (1) deposition of lower-bathyal, pre-isthmian, oceanic sediments in early Miocene time (21.5–18.5 Ma), represented by the Punta Alegre Formation; (2) growth of a volcanic arc during middle Miocene time (17–12 Ma) with subsequent development of an extensive volcanic archipelago characterized by columnar basalt and flow breccia, coarse-grained volcaniclastic deposits, and diverse coral reefs during late Miocene time (12–8 Ma); (3) extinction and subsidence of the volcanic arc during the latest part of Miocene time (8–5 Ma), resulting in a marine transgression, represented by the Tobabe and Nancy Point Formations of the lower Bocas del Toro Group; and (4) early Miocene regression in the upper Bocas del Toro Group, starting at ca. 5 Ma and culminating in the lower Pleistocene forereef limestone that composes the Swan Cay Formation (Coates et al., 1992; Coates and Obando 1996; Collins and Coates, 1999).

We present a formal lithostratigraphic description of the new units, followed by a biostratigraphic and radioisotopic analysis. We then reconstruct the geologic history of the rise of the Isthmus of Panama in the Bocas del Toro region by using paleobathymetric data from benthic foraminifera. The record from Bocas del Toro is compared with that of the Limón Basin in Costa Rica and the Panama Canal Basin and Darien region in eastern Panama.

## LITHOSTRATIGRAPHY

Lower and middle Miocene rocks of the Bocas del Toro Basin are everywhere overlain by the Bocas del Toro Group, a richly fossiliferous series of marginal-marine to upper-bathyal formations of latest Miocene to early Pleistocene age. The lithostratigraphy of the Bocas del Toro Group and the major micro- and macrofossil groups collected from the various formations within it have already been described by several authors (Collins and Coates, 1999, and references therein). The older Miocene rocks (Figs. 1, 2) are assigned to two new formations. (1) The lower Miocene Punta Alegre Formation consists of lower-bathyal clayey and silty ooze containing abundant calcareous nannofossils and benthic and planktic foraminifera (Tables 1, 2). It crops out only on the western tip of the Valiente Peninsula. (2) The Valiente Formation unconformably overlies the Punta Alegre Formation and crops out extensively on the Valiente Peninsula and nearby Popa Island.

The Valiente Formation is a lithologically complex and highly variable formation because it represents the suite of facies—marine and terrestrial, igneous and sedimentary—that is associated with active volcanic island arcs in tropical waters. It includes columnar basalt flows, basaltic flow breccia, pyroclastic tuff and ignimbrite, laharic breccia, fluviatile/estuarine conglomerate, coral-reef lenses, and marine debris flows. These facies intercalate and replace each other over very short distances, both laterally and vertically. The geographic and stratigraphic distribution of these lithofacies is shown in Figures 1–3. The basalt-lava and flow-breccia facies forms a core around which the other facies are distributed peripherally as terrestrial, coastal, or marine slope deposits.

### Punta Alegre Formation

The formation is named for the nearest village, Punta Alegre, and the prominent low bluffs that lie along the coast of the western limit of the Valiente Peninsula, north of Bluefield Bay form the stratotype (Llorona Hill Section, Figs. 3, 4A). They lie 1 km south of Bluefield Point (known locally as Punta Valiente) and 1.3 km northwest of the village of Punta Alegre (Fig. 1). This is the only exposure of the formation.

The formation is 19 m thick at the type locality, where a disconformable upper contact is marked by the scoured basal surface of the Valiente Formation and an overlying coarse-sand unit with up to 30-cm-diameter slumped blocks. Laterally, the Valiente Formation lies with up to 20° of angular unconformity on the Punta Alegre Formation (Fig. 4B). The lower contact of the Punta Alegre Formation is not exposed.

The Punta Alegre Formation consists of thin- to medium-bedded, gray-weathering, blue-green, siliceous, clayey siltstone and blocky mudstone (Fig. 4A). Harder, conchoidal-fracturing, 3–5-cm-thick horizons, spaced 5–20 cm apart, are common and are probably bentonitic. Many horizons contain very abundant, diverse, benthic and planktic foraminifera, but macrofossils and burrowing

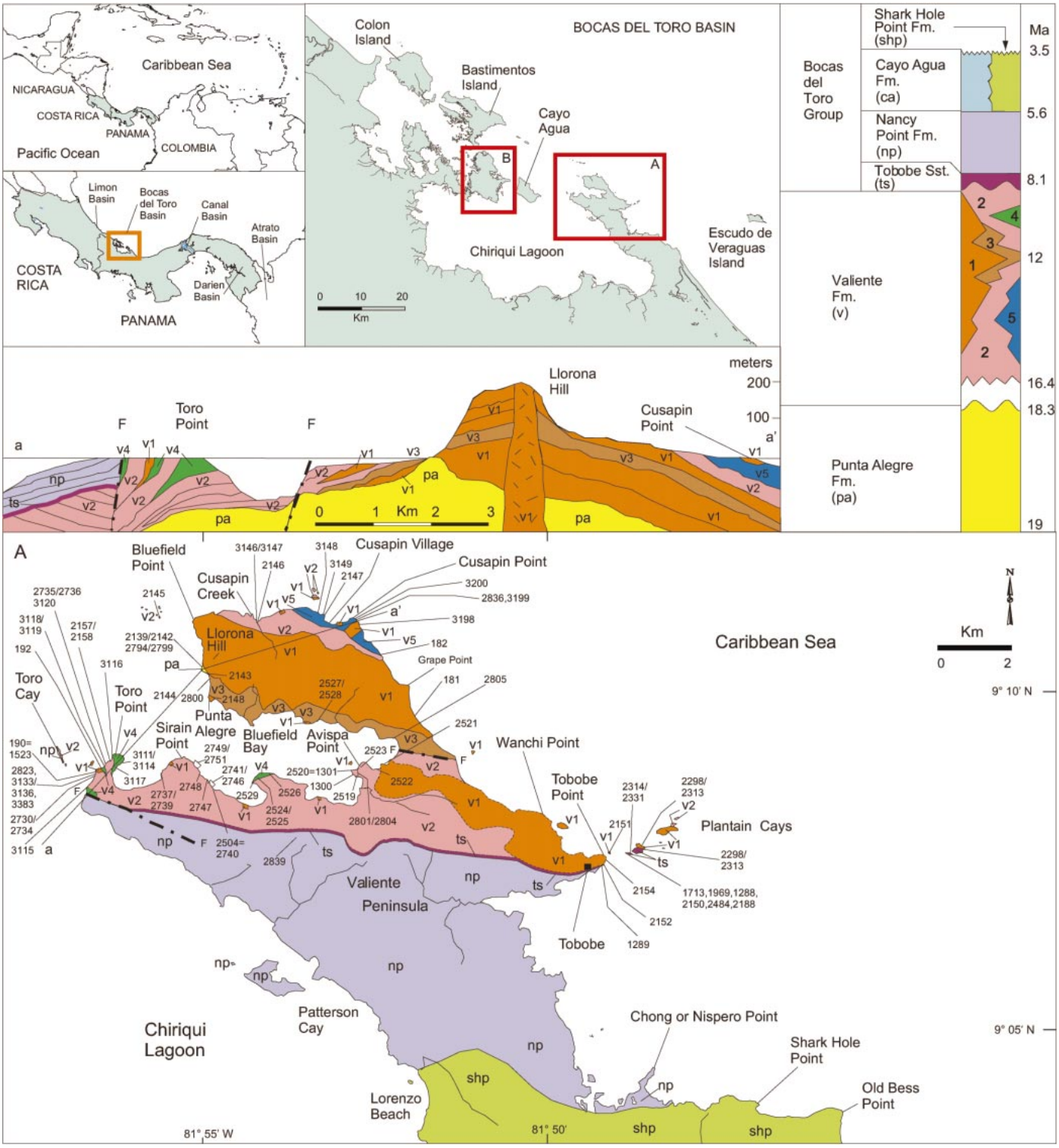


structures are absent. The Punta Alegre is interpreted to be a pre-isthmian lower-bathyal oceanic deposit; several horizons approach foraminiferal ooze in lithology.

**Valiente Formation**

The Valiente Formation is named for the Valiente Peninsula (Fig. 1) on which the formation crops out extensively. The stratotype stretches 270 m southwestward along the coast (Toro Point section, Fig. 3) from the northwest corner of Toro Point, Valiente Pen-

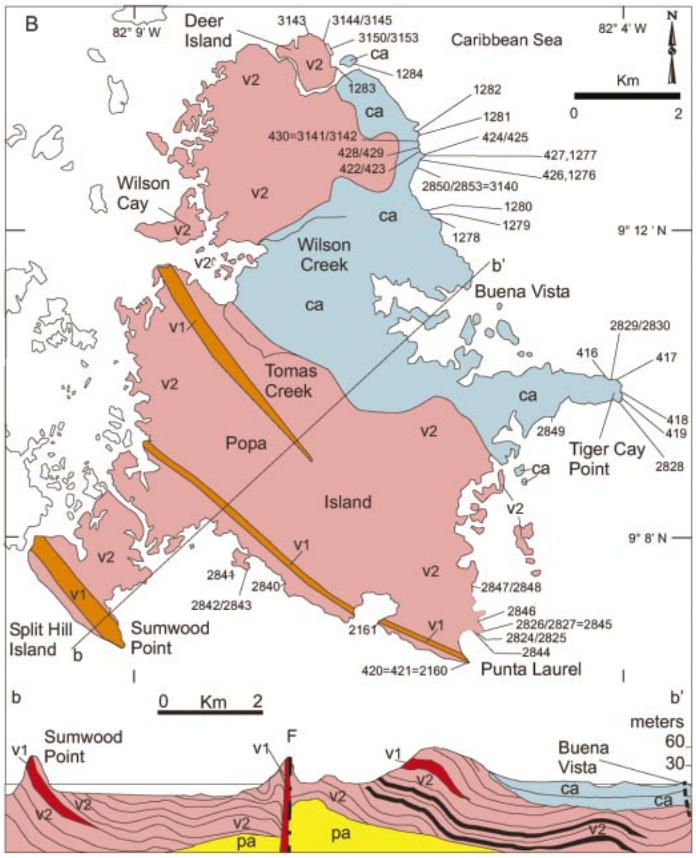


**Figure 2. Geologic map (located in Fig. 1) and section (b–b′; F—fault) showing the Valiente Formation on Popa Island, where the Valiente is unconformably overlain by the Pliocene Cayo Agua Formation (ca). Numbers and symbols as for Figure 1. On Popa Island, only the basalt-lava and flow-breccia facies (v1) and the coarse-grained volcaniclastic facies (v2; not associated with reef lenses) are present, apparently with thin layers of low-rank coal, an example of which is exposed along the coast immediately north of Punta Laurel. A prominent basalt dike is exposed at the tip of the Punta Laurel (here shown in red as v1 facies) where it cuts the Valiente Formation.**

insula. The formation is 135 m at the type section, but varies greatly across its outcrop. Additional reference sections include Llorona Hill (upper part), Avispa and Sirain Points, Cusapin Village and Cusapin Creek (Figs. 1, 3), Deer Island, and southeast Popa Island (Figs. 2, 3). The Valiente Formation overlies the Punta Alegre Formation with angular unconformity and is unconformably overlain by the Tobabe Formation, the basal unit of the Bocas del Toro Group. It is characterized by five lithofacies, described next.

### *Basalt-Lava and Flow-Breccia Lithofacies*

Basalt lava is commonly interbedded as thin flows in other lithofacies of the Valiente Formation, but it is the dominant lithology in the northern part of the Valiente Peninsula (Fig. 1), north of Bluefield Bay, and in the region of the Grape and Wanchi Points, Plantain Cays, and Tobabe Point. It also forms intercalated units in the type section of the Valiente Formation (Toro Point section, Fig. 3) along the western coast of the Toro Point peninsula. Lava flows vary from 2 to 3 m to several tens of meters in thickness and are commonly columnar, with columns averaging 20–30 cm in diameter. These columns are well displayed in the Plantain Cays, on the coast west of Cusapin and north of Punta Alegre (Fig. 1). The basalt is fine-grained, aphyric, or aphanitic, with up to 1-cm-long feldspar crystals, or holocrystalline and medium grained with pyroxene and plagioclase.

More commonly, basalt occurs as flow breccia up to 30 m thick (Fig. 4C). These breccia units are monomict, with a very wide range of clast sizes, ranging up to 30 cm on average, but with occasional blocks up to 50 cm, in a fine-grained basalt matrix. Flow breccia dominates the region around Sierra Llorona in the Valiente Peninsula, where flows are spectacularly exposed along the coast for 1 km to the south and 1 km to the east of Bluefield Point (locally known as Punta Valiente) and along the coast east of Cusapin (Fig. 1). They appear to be proximal flows radiating down the flanks of a vent center located near Llorona Hill (Fig. 1). The total thickness of the flows in this region is ~130 m.

### *Pyroclastic Lithofacies*

Along the northern shore of Bluefield Bay, for ~3 km eastward from Punta Alegre, immediately south of Llorona Hill, thin columnar basalt-lava and flow-breccia units are interbedded with white to cream, laminated to massive, tuffaceous sandstone, ashy tuff and fine breccia whose welded crystalline tuffaceous matrix suggests a pyroclastic origin.

### *Coarse-Grained Volcaniclastic Lithofacies*

This lithofacies consists of three subtypes. (1) Volcanic boulder conglomerate, in units up to 8 m thick, is strongly mud-matrix supported and has no trace of internal stratification; the conglomerate contains both rounded and angular clasts with an extreme size range from small pebbles to blocks 50 cm in diameter as well as some sandstone and basalt blocks 3–4 m in diameter. (2) Sandy, pebble breccia, up to 2 m thick, is distinctive. (3) Very coarse grained volcanic sandstone, ranging from 2 to 10 m thick, is distinctly bedded (although the bedding is streaky) and commonly contains scattered boulders up to 20 cm in diameter. The sandstone also contains lenses and channels of pebble breccia and cobble conglomerate (Fig. 4D); these depositional bodies bear mostly basalt clasts but also laminated sandstone, siltstone, and rip-up mudstone clasts. The sandstone units commonly have scoured bases and high-angled cross-beds.

The chaotic, matrix-supported boulder beds are interpreted as lahars because of the extreme size range of the clasts, the lack of internal bedding, and the absence of marine fossils. They commonly grade laterally or pass up into the streaky-bedded pebble breccia and more consistently stratified coarse-grained volcanic sandstone whose scoured horizons, high-angled cross-beds, and channels suggest a fluviatile origin. Local clayey siltstone lenses, with comminuted shell hash and a few turritellid gastropods and other mollusks, indicate periodic marginal-marine deposition. This sequence is interpreted as fluviatile reworking of the distal toes of lahars, perhaps in small deltas at the margin of active volcanic islands, given

TABLE 1.

| TAXA | Llorona Hill | | | | | | | | | | Sirain Pt. | | | | | | | | Avispa Pt. | | | | Cusapin Ck. | | Village | | | Toro Pt. | | | Deer West | | East | | Popa | | | | Bocas Group | | |
|---|---|---|---|---|---|---|---|---|---|---|---|---|---|---|---|---|---|---|---|---|---|---|---|---|---|---|---|---|---|---|---|---|---|---|---|---|---|---|---|---|---|
| | 3650 | 3651 | 3652 | 3653 | 3654 | 2800 | 3655 | 2795 | 2796 | 2797 | 2798 | 2799 | 2738 | 2739 | 2750 | 2749 | 2747 | 2746 | 2748 | 2504 | 2804 | 2803 | 2802 | 2801 | 3147 | 3146 | 3198 | 3200 | 2836 | 3148 | 2733 | 2732 | 2731 | 2730 | 3144 | 3145 | 3150 | 3151 | 3153 | 2846 | 2845 | 2826 | 2827 | 2844 | 2839 | 2850 | 2853 |
| **CALCAREOUS NANNO FOSSILS** | | | | | | | | | | | | | | | | | | | | | | | | | | | | | | | | | | | | | | | | | | | | | | |
| Calcidiscus leptoporus | | | | | | | | | | | | | | | X | | | | | | | | | | | | | | | X | | | | | | | | | | | | | | | | |
| Calcidiscus macintyrei | | | | | | X | | | | | | X | X | | X | | | X | | | | | | | | X | | | | | | | X | | | | | | | | | X | | | |
| Catinaster mexicanus | | | | | | | | | | | | | | | | | | | | | | | | | | X | | | | | | | F | F | | | | | | | | | | | |
| Coccolithus miopelagicus | | | | X | X | X | X | X | X | X | X | X | X | X | X | X | X | X | X | X | X | X | X | X | X | X | | X | X | | | | X | X | | X | X | | | | X | X | X | X | | | | |
| Coccolithus pelagicus | | | X | | X | | X | | | | | X | | | | | | | | | X | X | X | X | X | X | | | | X | | | | | X | X | X | | X | | | | | | | |
| Coronocyclus nitescens | | | | | | | | X | X | | X | | | | | | | | | | | | X | | | | | | | | | | | | | | | | | | | X | | | | | |
| Discoaster calculosus | | | | | | | | | | | | | | | | | | | | | | | | | | | | | | | | | | | | | | | | | X | X | | | | | |
| Discoaster challengeri | | | | | | | | | | | | | | | ● | | | | | | | | | | | | | | | | | | | | | | | | | | | | | | | | |
| Discoaster deflandrei | | | | | | | | | X | | | | | | | | | | | | | X | X | X | | | | | | | | | X | | | | | | | | | X | X | X | X | | | |
| Discoaster druggii | | | | | | | | C | | X | C | X | | | | | | | | | | | | | | | | | | | | | | | | | | | | | ● | | | | | | |
| Discoaster exilis | | | | | | | | | | | | | ● | ● | ● | | | | | | ● | | | | | ● | | | | | | | X | | | X | | | | | | | | | | | |
| Discoaster formosus | | | | | | | | | | | | | | | | | | | | | | | | | | | | | | | | | | | | X | | | | | | | | | | | |
| Discoaster musicus | | | X | | X | X̄ | | | | | | | | X | X | | | | | | | | | | X | | X | | X | | | | X | | X | | | | | | | | | | |
| Discoaster petaliformis | | | | | | | | | | | | | | | | | | | | | | | | | | | | | | | | | | | | X | | X | | | | | | | | |
| Discoaster tristellifer | | | | | | X | | | | | | | | | | | | | | | | | | | | | | | | | | | | | | | | | | | | | | | | |
| Discoaster variabilis | X | | | | | | | | | | | | X | X | X | | ● | | X | | | | | | | X | | | | X | | | X | | | | | | | | | | | | |
| Helicosphaera ampliaperta | | | | | | | R | X | X | X | X | X | | | | | | | | | C | F | F | C | | | | X | | C | | | | | | | | | | | | | | | |
| Helicosphaera carteri | X | | X | X | X | X | | | X | | | X | | | X | X | X | X | | X | X | X | X | X | X | X | X | X | X | X | | | X | X | X | | X | | X | | X | X | | X | | |
| Helicosphaera euphratis | | | | | | | | X | | X | X | X | | | | | | | | | | X | | | | | | | | | | | | | | | | | | | | | | | | |
| Helicosphaera intermedia | | | | | | | X | | | X | X | X | | | | | | | | | | X | | | | | | | | | | | X | X | | | | | | | | | | | |
| Helicosphaera gartneri | | | | | | | | | | | | | | | | | | | | | | | X | | | | | | | | | | | | | | | | | | ● | | X | | | |
| Helicosphaera scissura | | | | | | | | | | | | | | | | | | | | | ● | | | | | | | | | | | | | | | | | | | | | | | | |
| Holodiscolithus macroporus | | | | | | | | | | | | | | | | | | | X | | | | | | | | | | | | | | | | | | | | | | | | | | |
| Lithostromation perdurum | | | | | | | | | | | | | | | | | | | | | | | | | | X | | | | | | | | | | | | | | | | | | | |
| Pontosphaera discopora | X | | | X | X | X | | | X | | | X | | | | | X | X | X | | | | X | | | X | | | | X | | | X | X | | | X | | | X | X | | X | | |
| Pontosphaera japonica | | | | | | | | | | | | | | | | | X | | | | | | | | | X | | | | | | | X | | | | | | | | | | | |
| Reticulofenestra abisecta | X | | | | | | X | | | | | | | | | | | | | | | | | | | | | | | | | | | | | | | | | | | | | | |
| Reticulofenestra floridana | X | | X | X | | | X | X | X | X | X | X | X | | | | X | | X | X | | X | X | X | | X | | | | | | | X | | | X | | | | | X | X | X | X | | |
| Reticulofenestra gartneri | | | | | | | | | | | | | | | | | | | | | | | | | | | | | | | | | | | | | | | | | | X | X | X | | | |
| Reticulofenestra pseudoumbilicus | X | | | | X | X | X | X | X | X | X | X | X | X | X | X | X | X | X | X | X | | X | X | X | X | X | X | | X | | | X | X | X | X | | X | | | | X | | | | |
| Sphenolithus abies | | | | | | | X | X | | | | ● | | | | | | | | | | | | | | | | | | | | | | | | | | | | | | | | | | |
| Sphenolithus belemnos | | | | | | | R | | C | 1 | | ● | | | | | | | | | | | | | | | | | | | | | | | | | | | | | | | | | | |
| Sphenolithus conicus | | | | | | | | | | | | | | | | | | | | | | | | | | | | | | | | | | | | | | | | | X | X | X | | | |
| Sphenolithus disbelemnos | | | | | | | | R | F | F | F | R | | | | | | | | | | | | | | | | | | | | | | | | | | | | | | | | | | |
| Sphenolithus dissimilis | | | | | | | | X | | X | X | X | | | | | | | | | | | | | | | | | | | | | | | | | | | | | | | | | | |
| Sphenolithus heteromorphus | X | | X | X | X | X | X | | + | | | | | | | | | | | | C | C | C | C | | | | X | | F | | | + | | | X | | X | | | | | | | |
| Sphenolithus neoabies | | | | | | | X | X | | X | X | X | X | | X | | X | | X | | | | X | X | | X | | | | X | | | | X | | | | X | | X | X | X | | | | |
| Triquetrorhabdulus carinatus | | | | | | | | + | | | | | | | | | | | | | | | | | | | | | | | | | | | | | | | | | | | | | | |
| Triquetrorhabdulus milowii | | | | | | | | | | | | | | | | | | | | | ● | | X | | | | | | | | | | X | X | X | | | | | | | | | | | |
| Triquetrorhabdulus rugosus | | | | | | | | | | | | | | | | | | | | | | | | | | X | | | | | | | X | | | | | | | | | | | | |
| Triquetrorhabdulus serratus | | | | | | X | | C | X | | | | | | | | | | | | | | | | | | | | | | | | | | | | | | | | | | | | | |
| Umbilicosphaera cricota | | | | | | | | | | | | | | | X | | | | | | | | | | | X | | | | | | | | | | | | | | | | | | | | |
| Scyphosphaera spp. | | | X | | | | | | | | | | | | | | | | | | | | | | | | | | | | | | | | | | | | | | | | | | | |
| **PLANKTONIC FORAMINIFERA** | | | | | | | | | | | | | | | | | | | | | | | | | | | | | | | | | | | | | | | | | | | | | | |
| Catapsydrax dissimilis | | | | | | | | X | | X | X | | | | | | | | | | | | | | | | | | | | | | | | | | | | | | | | | | | |
| Catapsydrax stainforthi | | | | | | X | | X | X | | | | | | | | | | | | | | | | | | | | | | | | | | | | | | | | | | | | | |
| Globigerina spp. | | X | | | | | | | | | | | | | | | | | | | | | | | | | | | | X | | | | | | | | | | | | | X | | | |
| Globigerinella obesa | | | | | | | | | | | | | | | | | | | | | | | | | | | | | | | | | X | | | | | | | | | | | | | |
| Globigerinella praesiphonifera | | | | | | X | | | | | | | | | | | | | | | | X | | X | | X | | | | | | | | | | | | | | | | | | | |
| Globigerinella pseudobesa | | | | | | | | | | | | | | | | | | | | | | | | | | | | | | | | | | | | | | | | | | | | | X | | |
| Globigerinoides spp. | | X | | | | | | | | | | | | | | | | | | | | | | | | | | | | | | | | | | X | | | | | | | | X | | |
| Globigerinoides altiapertura | | | | | | | | | | | | | | | | | | | | | | X | | X | | | | | | | | | | | | | | | | | | | | | | |
| Globigerinoides bisphaericus | | | | | | X | X | | X | | | | | | | | | | | | | X | | | | | | | | X | | | | | | | X | | | | | | | | | |
| Globigerinoides conglobatus | | | | | | | | | | | | | | | | | | | | | | | | | | | | | | | | | | | | | | | | | | | | | | |
| Globigerinoides extremus | | | | | | | | | | | | | | | | | | | | | | | | | | | | | | | | | | | | | | | | | | | | X | X | | |
| Globigerinoides obliquus | | | | | | | | | | | | | | | | | | | | | | | | | | | | | | | | | | | | | | | | | | | | | | |
| Globigerinoides subquadratus | | | | | | X | | | | | | | | | | | | | | | | X | | | | | | | | | | | | | | | | | | | | | | | |
| Globigerinoides trilobus | X | | | X | | X | | | | | | X | | | | | | | | | | X | | X | | X | | | X | | X | X | X | | X | | X | X | | | X | X | X | X | | |
| Globoquadrina sp. | | | | | | | | | | | | X | | | | | | | | | | | | | | | | | | | | | | | | | | | | | | | | | | |
| Globoquadrina altispira | X | | | X | X | X | X | X | | | | | | | | | | | | | | X | | | | X | | | | X | X | X | | ● | X | X | X | | | X | | | X | | | |
| Globoquadrina baroemoenensis | | | | | | | | | | | | | | | | | | | | | | X | | X | | | | | | | | | | | | | | | | | | | | | | |
| Globoquadrina dehiscens | | | | X | X | X | | | | | | | | | | | | | | | | X | | | | X | | | | X | | | | | | | | | | | | X | | | |
| Globoquadrina venezuelana | | | | | | X | | | | | | | | | | | | | | | | | | | | X | | | | | | | | | | X | X | | | | X | | | | |
| Globorotalia archeomenardii | | | | X | X | X | | | | | | | | | | | | | | | | | | | | | | | | | | | | X | | | | | | | | | | | |
| Globorotalia birnageae | | | | | | X | X | | | | | | | | | | | | | | | X | | X | | | | | | | | | | | | | | | | | | | | | |
| Globorotalia foshi foshi | | | | | | | | | | | | | | | | | | | | | | | | | | | | | | | | | | X | | | | | | | | | | | | |
| Globorotalia partimlabiata | | | | | | | | | | | | | | | | | | | | | | | | | | X | | | | | | | | | | | | | | | | | | | | |
| Globorotalia peripheroacuta | | | | | | | | | | | | | | | | | | | | | | | | | | X | | | | | | | | | ● | | | | | | | | | | | |
| Globorotalia peripheroronda | | | | X | X | X | X | | | | | | | | | | | | | | | X | | X | | | | | | | | | | | | | | | | | | X | | | | |
| Globorotalia plesiotumida | | | | | | | | | | | | | | | | | | | | | | | | | | | | | | | | | | | | | | | | | | | | | X | | |
| Globorotalia praefoshi | | | | | | | | | | | | | | | | | | | | | | | | | | | | | | | | | | X | | X | | | | | | | | | | |
| Globorotalia praescitula | | | | | | X | | | | | | | | | | | | | | | | X | | X | | | | | | | | | | | | | | | | | | | | | |
| Globorotalia premenardii | | | | | | | | | | | | | | | | | | | | | | | | | | X | | | | | | | | | | | | | | | | | | | | |
| Globorotalia pseudomiocenica | | | | | | | | | | | | | | | | | | | | | | | | | | | | | | | | | | | | | | | | | | | | X | | |
| Globoturborotalita nepenthes | | | | | | | | | | | | | | | | | | | | | | | | | | | | | | | | | | | | | | | | | | | | | | ● |
| Neogloboquadrina acostaensis | | | | | | | | | | | | | | | | | | | | | | | | | | | | | | | | | | | | | | | | | | | | | | |
| Orbulina spp. | | | | | | | | | | | | | | | | | | | | | | | | | | | | | | | | | | | | | X | | | | | | | | | | |
| Orbulina suturalis | X | | X | X | X | | | | | | | | | | | | | | | | | | | | | X | | | | | X | X | | | | X | | | | | | | | | |
| Orbulina universa | | | | | | | | | | | | | | | | | | | | | | | | | | | | | | | | | | | | | | | | | | | | X | | |
| Paragloborotalia bella | | | | | | | | | | | | | | | | | | | | | | | | | | | | | | | | | | | | | | | | | | | | | | |
| Paragloborotalia mayeri | X | | X | X | X | X | X | | | | | | | | | | | | | | | | | X | | | | | | X | | | X | | ● | X | | | | | X | | | | |
| Praeorbulina circularis | X | ● | X | X | X | X | | | | | | | | | | | | | | | | | | | X | | | | | | | | | | | | X | X | | | | | | | |
| Praeorbulina curva | | | | | | X | | | | | | | | | | | | | | | | | | | | | | | | | | | | | | | | | | | | | | | | |
| Praeorbulina glomerosa | | | | | | X | | | | | | | | | | | | | | | | | | | | | | | | | | | | | | | | | | | | | | | | |
| Praeorbulina sicana | | | | | | X | | | | | | | | | | | | | | | | X | | X | | | | | | | | | | | | | | | | | | | | | |
| Sphaeroidinellopsis spp. | X | | | | | | | | | | | | | | | | | | | | | | | | X | | | | | | | | | | | | | | | | | | X | X | | |

the common intercalation, within this lithofacies, of thin (1–2 m thick), basaltic flow breccias.

South of Toro Point, along the west coast of the peninsula (Toro Point section, Fig. 3), the coarse-grained volcaniclastic facies is found intercalated with basaltic flow breccia, 3–5 m thick, that is presumably distal because thin reef lenses are also locally present. Good exposures are also seen, without reef lenses, along the northern margin of the Valiente Peninsula between Cusapin Creek and the village of Cusapin as well as along

TABLE 2.

| BENTHIC FORAMINIFERA | Llorona Hill | | Avispa Point | Cusapin Creek Village | | | Toro Point | | Deer, East | Popa Island | | | | | | | Bocas Group | | |
|---|---|---|---|---|---|---|---|---|---|---|---|---|---|---|---|---|---|---|---|
| | 2800 | 2796 | 2803 | 3146 | 2836 | 3148 | 2731 | 2730 | 3151 | 2846 | 2845 | 2825 | 2827 | 2828 | 2852 | 2844 | 2839 | 2850 | 2853 |
| Ammonia beccarii | | | | | X | | | | | | | | | | | | | | |
| Amphistegina gibbosa | | | X | | | | | | | | | | X | | | | X | | X |
| Bigenerina irregularis | | | | | | | | | | | | | | | X | | | | |
| Biloculina | | | | | | | | | | | | | | | | | | | X |
| Bolivina byramensis | | | X | X | | | | | | | | | | | | | | | |
| Bolivina imporcata | | | | | | | X | X | | | | | | | X | | X | | |
| Bolivina inflata | | | | | | X | X | | | | | | | | | | | | |
| Bolivina marginata | X | X | | X | | X | X | X | X | X | | | X | | | X | | | |
| Bolivina subaenariensis mexicana | | | | | | | | | | | | | | | X | | X | X | |
| Bolivina subexcavata | | | | | | | | | | | | | | | | | | X | |
| Bolivina pisciformis | | | | | | X | | X | | | | | | | | | | | |
| Bolivina plicatella | | X | X | | | X | | | | X | | | | | X | | | | |
| Bolivina striatula | | | | | | | | | | | | | | | X | | | X | |
| Bolivina subaenariensis | | | | | | | | | | | | | | | | | | X | |
| Bolivina tortuosa | | | X | | | | | | | | | | | | | | X | | |
| Bulimina alazanensis | X | X | | X | | X | | | X | X | | | | | | | | | |
| Bulimina ovata var. primitiva | | | | | | | | X | X | | | | | | | | | | |
| Bulimina mexicana | | X | X | X | X | X | X | X | X | X | | X | X | | | X | X | | |
| Buliminella elegantissima | | | | | | | | | | X | | | | | | | | | |
| Buliminella curta | | | | | | | X | X | | | | | | | | | | X | |
| Cassidulina carapitana | | | X | X | | X | X | X | X | | | | | | | | | | |
| Cassidulina corbyi | | X | | | | | | | | | | | | | | | | | |
| Cassidulina laevigata | X | X | X | X | X | X | X | X | | X | | | | | X | | X | | |
| Cassidulina norcrossi australis | | | | | | | | | | | | | | | | | X | | |
| Cassidulina palmerae | | | X | | | | | | | | | | | | | | | | |
| Cassidulina punctata | | | | | | X | | | | | | | | | | | | | |
| Cassidulina subglobosa | X | X | X | X | X | X | | X | X | X | X | X | X | | X | X | X | X | |
| Cassidulinoides bradyi | | X | | X | | X | X | X | | X | | | | | | | | | |
| Ceratobulimina alazanensis | X | | X | | | X | | | | | | | | | | | | | |
| Cibicidoides crebbsi | | | | X | | X | X | X | | | | | | | | | | | |
| Cibicidoides compressus | | | | | | | X | X | | | | | | | | | X | | |
| Cibicidoides matanzasensis | | | | | | | | | | | | | | | | | | | |
| Cibicidoides mundulus | | | | | | | | | | | X | | | | | X | | | |
| Cibicidoides wuellerstorfi, typical | X | | | | | | | | X | | | | | | | | | | |
| Cibicidoides wuellerstorfi var. harangensis | X | | | X | | X | | | X | | | | | | | | | | |
| Cibicidina walli | X | | | | | X | | | | | | | | | | | | | |
| Cibicorbis herricki | | | | | X | | | | | | | | | | | | | | |
| Compressigerina coartata | | | X | | | | | | | | | | | | | | | | |
| Fursenkoina pontoni | | | X | | | | | X | | | | | | | | | | | X |
| Gyroidina regularis | | | X | X | | X | X | | | | | | | | X | | X | | |
| Gyroidina umbonata | X | X | | | | | | X | | X | | | | | X | | | | |
| Gyroidinoides altiformis | X | X | | | | X | | X | X | | | | | | | X | | | |
| Gyroidinoides octocamerata | X | | | X | | X | | | X | X | X | X | X | | | | | | |
| Gyroidinoides venezuelana | | | | | | | X | X | | | | X | | | | | | | |
| Hanzawaia concentrica | X | X | X | X | X | X | X | X | | X | X | | | | X | | X | X | X |
| Hanzawaia mantaensa | | | | | | | X | X | | | X | | | | | | | | |
| Hanzawaia isidroensis | | | X | X | | | X | X | X | | X | | | | X | | X | | X |
| Hoeglundina elegans | | | X | X | | X | X | X | | | | | | | | | X | | |
| Karreriella chapapotensis | X | | | | | | | | | | | | X | | | | | | |
| Laticarinina pauperata | X | | | | | X | | | X | | | | | | | | | | |
| Lenticulina calcar | X | | X | X | X | X | X | X | X | | X | X | | | | X | | | |
| Lenticulina clericii | X | X | | | | | X | | | | | | X | | | | | | |
| Lenticulina peregrina | | | | | | X | | | | | | | | | | | | | |
| Liebusella pozonensis crassa | | X | | | | | | | | | | | | | | | | | |
| Martinotiella pallida | | | | X | | X | X | X | | | | | | | | | | | |
| Melonis barleeanum | | | X | | | | | X | X | | | | | | | | | | |
| Melonis pompilioides | X | X | | X | | X | X | X | | | X | X | X | | | X | | | |
| Melonis sphaeroides | | X | | | | | | | | | | | | | | | | | |
| Neoeponides antillarum | | | | | X | | | | | | | | | X | X | | | | X |
| Nonionella basiloba | | | | | | | X | X | | | | | | | | | | X | |
| Nonionella grateloupi | | | | | | | | | | | | | | | | | | X | |
| Nonionella incisa | | | X | | | | X | X | | | | | | | | | | X | X |
| Nonionella obducta | | | | | | | | | | | | | | | X | | | X | |
| Oridorsalis umbonatus | X | X | X | X | | | X | X | | X | X | | | | | | | | |
| Planularia clara | | | | | | | | X | | | | | | | | | | | |
| Planularia venezuelana | | | X | | | X | | | | | | | | | | | | | |
| Planulina charapatoensa | | | | | | | X | X | | | | | | | | | | | |
| Planulina subtenuissima | | | | | | X | | | | | | X | X | | | X | | | |
| Plectofrondicularia californica | X | | | X | | X | X | X | X | X | | | | | | | | | |
| Plectofrondicularia parri | | | | | | | | X | | | | | | | | | | | |

TABLE 2. (*Continued.*)

| BENTHIC FORAMINIFERA | Llorona Hill | | Avispa Point | Cusapin Creek Village | | | Toro Point | | Deer, East | Popa Island | | | | | | | Bocas Group | | |
|---|---|---|---|---|---|---|---|---|---|---|---|---|---|---|---|---|---|---|---|
| | 2800 | 2796 | 2803 | 3146 | 2836 | 3148 | 2731 | 2730 | 3151 | 2846 | 2845 | 2825 | 2827 | 2828 | 2852 | 2844 | 2839 | 2850 | 2853 |
| Plectofrondicularia vaughani | | | x | | | x | x | x | | | | | x | | | | | | |
| Pullenia bulloides | x | x | | | | x | | | | x | x | | x | | | | | | |
| Pullenia quinqueloba | | x | | | | | | | | | | | x | | | | | | |
| Quinqueloculina lamarckiana | | | | | x | | | | | | | | | x | | | | | x |
| Rectuvigerina multicostata | x | x | | | | x | | | | | x | | | | | | | | |
| Reussella atlantica | | | | | | | | | | | | | | | x | | | | |
| Rosalina subaraucana | | | | x | x | | x | x | | | | | | | | | | | |
| Rotalia garveyensis | x | | x | | | x | x | x | x | x | | | | | x | x | x | x | x |
| Sigmoilina tenuis | | | | | | x | x | | x | | | | | | | | x | | |
| Sigmoilopsis schlumbergeri | | | | | | | | | | | | | | | | | x | | |
| Siphogenerina lamellata | | | x | | | | x | x | | | x | | | | | | x | | |
| Siphogenerina transversa | x | | | x | | x | | | x | | | | | | | | | | |
| Siphonina pulchra | | | x | | | | | | | | | | x | | | | | | |
| Siphonina tenuicarinata | x | | | | | x | | | x | | x | x | | | | x | | | |
| Siphonodosaria spp. | x | x | x | x | | x | x | x | x | x | x | x | x | | | x | | | |
| Sphaeroidina bulloides | x | x | x | x | | x | | x | x | | x | | x | | | x | | | |
| Stilostomella sp. | | x | | | | | | | | | | | | | | x | | | |
| Trifarina bradyi | | | | x | | x | | | | | | | | | | | | | |
| Trifarina carinata | | x | | | | | | | | | | | | | | | | | |
| Trifarina eximia | | | | | x | | | | | | | | | | | | | | |
| Uvigerina carapitana | x | | x | | | x | | | | | | | | | | | | | |
| Uvigerina laevis | x | | | x | | x | | | x | | | | | | | | x | x | |
| Uvigerina mantaensis | | x | | | | | | | | | | | | | | | | | |
| Uvigerina mexicana | | | | | | x | | | | | | | | | | | | | |
| Uvigerina pigmaea | x | x | x | x | | | x | x | x | | x | | | | x | | x | x | |
| Uvigerina rugosa | x | x | | x | | x | | | x | | x | | x | | | | | | |

the northern margin of the Plantain Cays (Fig. 1).

### *Coral-Reef Lithofacies*

At several points on the Toro Point peninsula (Fig. 1), small reef limestone lenses (Fig. 4E) are intercalated with the coarse-grained volcaniclastic and basaltic flow-breccia lithofacies. The most extensive reef limestone unit covers the northern tip of the Toro Point peninsula (Toro Point section, Fig. 3) and consists of thick-bedded, rubbly, bioclastic, cream-weathering, pale blue limestone that contains volcanic sand and silt grains in varying amounts. The limestone is ~37 m thick and has interbeds up to 6 m thick of volcanic-cobble conglomerate with well-rounded clasts and a graywacke matrix. Large coral colonies up to 50 cm in diameter, including *Montastraea*, *Porites*, *Stylophora*, and *Diploria*, are common at several levels. Other similar, coral-rich, reef-rubble units can be observed ~100 m to the south along the western coast of the Toro Point peninsula. These deposits appear to represent local reef buildups of limited lateral and vertical extent, fringing active volcanic islands.

### *Marine Debris-Flow and Turbidite Lithofacies*

This distinctive lithofacies is well developed immediately to the west and east of Cusapin on the north coast of the Valiente Peninsula (Fig. 1). To the east of Cusapin, starting at Cusapin Point (Cusapin Village section, Fig. 3) and continuing east for ~1.3 km, the units consist of steeply dipping, thick-bedded (up to 2 m thick), coarse-grained polymict breccia and boulder conglomerate, all matrix supported. The matrix is coarse, blue-green graywacke and siliceous mudstone in which ''floats'' a chaotic array of very coarse grained boulder- to pebble-sized blocks. The clasts are dominantly basalt, including up to 1-m-long segments of well-formed hexagonal basalt columns and up to 60–80 cm diameter blocks of laminated and convolute-bedded coarse-grained sandstone, pebble breccia, and laminated to thin-bedded siltstone and lignite. At several places, the matrix contains ahermatypic corals, echinoids (spines), algal (*Archeolithothamnion*?) balls and scattered mollusks, including conid and olivid gastropods. These very coarse grained boulder beds are interbedded with well-laminated, cross-bedded, coarse-grained volcanic sandstone and thick-bedded graywacke, which also contain mollusks.

The association of very large, unabraded, polymict clasts and perfectly preserved segments of hexagonal basalt pillars in a supporting matrix of upper-bathyal graywacke, with associated shallow- and deep-water organisms, strongly suggests rapid resedimentation. The coarse-grained fluviatile, laharic, and marginal-marine volcaniclastic deposits appear to have been redeposited as debris flows into nearby deep water on the steep, unstable, submarine slopes of the volcanic island arc.

To the west of Cusapin, these boulder beds are less common and are associated with more typical turbidite sequences (Fig. 4F) that are well exposed at the point that forms the western limit of Cusapin harbor and along the coast extending ~5 km to the west. Turbidite units range from 1 to 15 cm thick and weather in places a sulfurous yellow. Blue-gray, siliceous and carbonaceous blocky mudstone alternates with finely and sometimes sublenticularly laminated sandstone units that have scoured bases. At Toro Point, pebble breccia packed with wood fragments is common as are intraformational slumps (Fig. 4F).

On Popa Island the Valiente Formation is intruded by basalt dikes. At Punta Laurel (Fig. 2) the dike yielded $^{40}Ar/^{39}Ar$ ages of 8.4 ± 0.5 and 8.5 ± 0.6 Ma.

## BIOSTRATIGRAPHY

### Punta Alegre Formation

Both planktic foraminifera and calcareous nannofossils point to an early Miocene (Burdigalian) age (ca. 18.3–19 Ma) for the Punta Alegre Formation. Six sites (PPP2794–PPP2799) in the lower part of the Llorona Hill section (Fig. 3) yielded a rich and well-

preserved planktic foraminiferal fauna dominated by globoquadrinids, *Globigerinoides trilobus*, *Catapsydrax dissimilis*, and *C. stainforthi*. This fauna is suggestive of Zones N5–N6 (ca. 17–21 Ma). Calcareous nannofossils are common and moderately well preserved. Common species include *Reticulofenestra floridana*, *R. pseudoumbilicus*, *Coccolithus pelagicus*, and *C. miopelagicus*, *Helicosphaera carteri*, *Sphenolithus* spp. and *Discoaster* gr. *deflandrei*. Assignment of the section to Biozone(s) NN2 or NN3 is based on the occurrences of *Discoaster druggi*, *Sphenolithus disbelemnos* (in all samples), and *Sphenolithus belemnos* (common and characteristic only at site PPP2796). Although the LO of *D. druggi* defines the base of Zone NN2, the lowest occurrence of the two *Sphenolithus* species are located in upper Zone NN2. In addition, two fragments (pristine) of *Triquetrorhabdulus carinatus* (whose highest occurrence defines the top of Zone NN2) were found at site PPP2795. Because of the extreme scarcity of *T. carinatus* (at site PPP2795), it is uncertain whether this interval belongs to Zone NN2 or NN3. However, the co-occurrence of *S. disbelemnos* and *S. belemnos* restricts the age of the Punta Alegre Formation as represented in the Llorona Hill section to not older than the upper part of Zone NN2 (ca. 19.5 Ma) and not younger than Zone NN3 (ca. 18.3 Ma).

**Valiente Formation**

The oldest deposits of the Valiente Formation are found in the 40-m-thick section of resedimented shelly bioclastic limestone, mudstone, and conglomerate at Avispa Point (Figs. 1, 3). They belong to Zone NN4 (entire section) and Zone N8 (= M5a; lower part of the section). The four sites (PPP2801–PPP2804) examined for calcareous nannofossils, taken at regularly spaced levels throughout the outcrop, yielded sparse, low-diversity assemblages with *Helicosphaera ampliaperta* (common) and *Sphenolithus heteromorphus*, whose concurrent ranges define Zone NN4 (ca. 18.2–15.6 Ma). Together with *R. pseudoumbilicus*, *D. deflandrei*, *C. miopelagicus*, *Discoaster* cf. *D. exilis* and the planktic foraminifera *Globorotalia peripheroronda*, *G. birnageae*, *Globigerinoides sicanus*, *G. bisphericus*, and *G. altiaperturus* (sites PPP2801, PPP2803), these taxa indicate Zone N8 (= M5a) and yield an estimated age of 16.4–16.1 Ma for the lower ~15 m of the Avispa Point section.

A slightly younger age (ca. 15.6–16.1 Ma) is estimated for the turbiditic sequence at Cusapin Village (Figs. 1, 3). The section is referable to Zones NN4 (entire section) and N8 (= M5b; lower part of the section). Calcareous nannofossils are common in site PPP3148 and rare in site PPP3200. Zonal assignment to Zone NN4 is firm, based on the co-occurrence of *H. ampliaperta* and *S. heteromorphus*. The occurrence of *Praeorbulina circularis* and the absence of true orbulinids in site 3148 indicate an early middle Miocene (early Langhian) age.

Slightly younger rocks overlie the Punta Alegre Formation in the Llorona Hill section (Fig. 3). The uppermost part of the section belongs to Zone NN5 (sites PPP3650–PPP3654; 15.6–13.6 Ma) as indicated by the occurrence of nannofossil *S. heteromorphus* and the absence of *H. ampliaperta*. Sites PPP3650–PPP3655 also yielded the planktic foraminifera *Praeorbulina circularis*, *P. glomerosa* (as well as true orbulinids), *Globigerinoides bisphericus*, *G. sicanus*, *G. peripheroronda*, *Globorotalia archeomenardii*, *and G. praescitula*. These taxa are assignable to Zone N9 (ca. 15.1–14.8 Ma). Site PPP2800, located 2–3 m below PPP3654, also contains a Zone NN5 nannofossil assemblage, and its similar planktic foraminiferal assemblage resembles the overlying sites, but it does not yield true orbulinids and is therefore assigned to uppermost Zone N8 (M5b; ca. 15.1–15.5 Ma). Site PPP3655 is located 14 m stratigraphically lower than PPP2800, with an angular unconformity between, and yields abundant calcareous nannofossils although the zonal markers are rare. The co-occurrence of *S. heteromorphus*, *S. belemnos*, and *H. ampliaperta* in PPP3655 may suggest a stratigraphic position near the NN3/NN4 (ca. 18.2 Ma) zonal boundary. It is unclear, however, whether the ranges of *S. belemnos* and *S. heteromorphus* overlapped, and it may be that the co-occurrence is due to reworking, particularly since the late Paleogene species *Reticulofenestra bisecta* is common. Indeed, provisional planktic foraminiferal assignment to Zone N8 would support reworking. Site PPP3655 contains *Paragloborotalia mayeri*, *Globoquadrina altispira*, *G. cf. birnageae*, and *G. bisphericus*. In the absence of praeorbulinids (Zone N8) and catapsydracids (highest occurrence at the top of Zone N7), this site is probably referable to a level stratigraphically correlative with Zone N8. Thus, the upper part of the Llorona Hill section spans the N8/N9 zonal boundary.

The section at Cusapin Creek (Figs. 1, 3) is middle Miocene (Serravallian, ca. 13.6–12.7 Ma) and notably younger than any of the sections described so far in this paper. Site PPP3146, located toward the base of the section, yields common calcareous nannofossils with frequent *R. pseudoumbilica* and *C. miopelagicus* and rare, poorly preserved discoasters. The co-occurrence of *Triquetrorhabdulus rugosus*, *Discoaster musicus*, *C. miopelagicus*, and *Catinaster mexicanus* suggests Zone NN6 (ca. 13.6–12.7 Ma). The planktic foraminifera from the same site, with *Globorotalia peripheroacuta*, *G. partimlabiata*, *Orbulina suturalis*, *Globoquadrina dehiscens*, and *G. venezuelana*, characterize Zone N10 (ca. 14.8–12.7 Ma).

The age of the Sirain Point section is poorly defined. The planktic foraminifera are silicified and the calcareous nannofossil assemblages are poorly preserved and of low diversity. The occurrence of *C. miopelagicus*, *D. musicus*, and *D. exilis* (without *S. heteromorphus*) indicates an interval correlative with Zones NN6–NN8 (ca. 13.6–11.2 Ma).

The youngest rocks of the Valiente Formation occur at the type locality at Toro Point (Figs. 1, 3) in the Valiente Peninsula. Mudstone alternating with fine-scale turbidites (PPP3134, PPP3136, PPP2730/PPP2731; slashes indicate site number ranges) span ~3.1 m.y. of the middle Miocene from Zone N8/M5b (15.5–15.2 Ma) to Zone N11/M8 (12.7–12.5 Ma). However, on biostratigraphic evidence, we suspect the presence of an unconformity near the base of the section within the 3 m interval between sites PPP3136 (Zone N8 = M5b) and PPP2730 (Zone N11). Calcareous nannofossils occur only at sites PPP2730 and PPP2731. The co-occurrence of *T. rugosus* (lowest occurrence in Zone NN6) and *T. milowii* (highest occurrence in Zone

**Figure 3. Geochronological relationships of the principal sections measured in the Punta Alegre Formation and the Valiente Formation. Numbers represent PPP sites analyzed, and columns give the ranges of biostratigraphically useful nannofossils (white) and planktic foraminifera (black). Sections are located on Figure 1; numbers 1–5 (in boxes adjacent to sections) refer to lithofacies of the Valiente Formation described in the text. (There is no pattern in the symbol key for v3 as it does not crop out along the line of the section.) Crosses in the Llorona Hill and Toro Point sections represent $^{40}Ar/^{39}Ar$ dates of basalt lavas (for exact ages, see Fig. 6).**

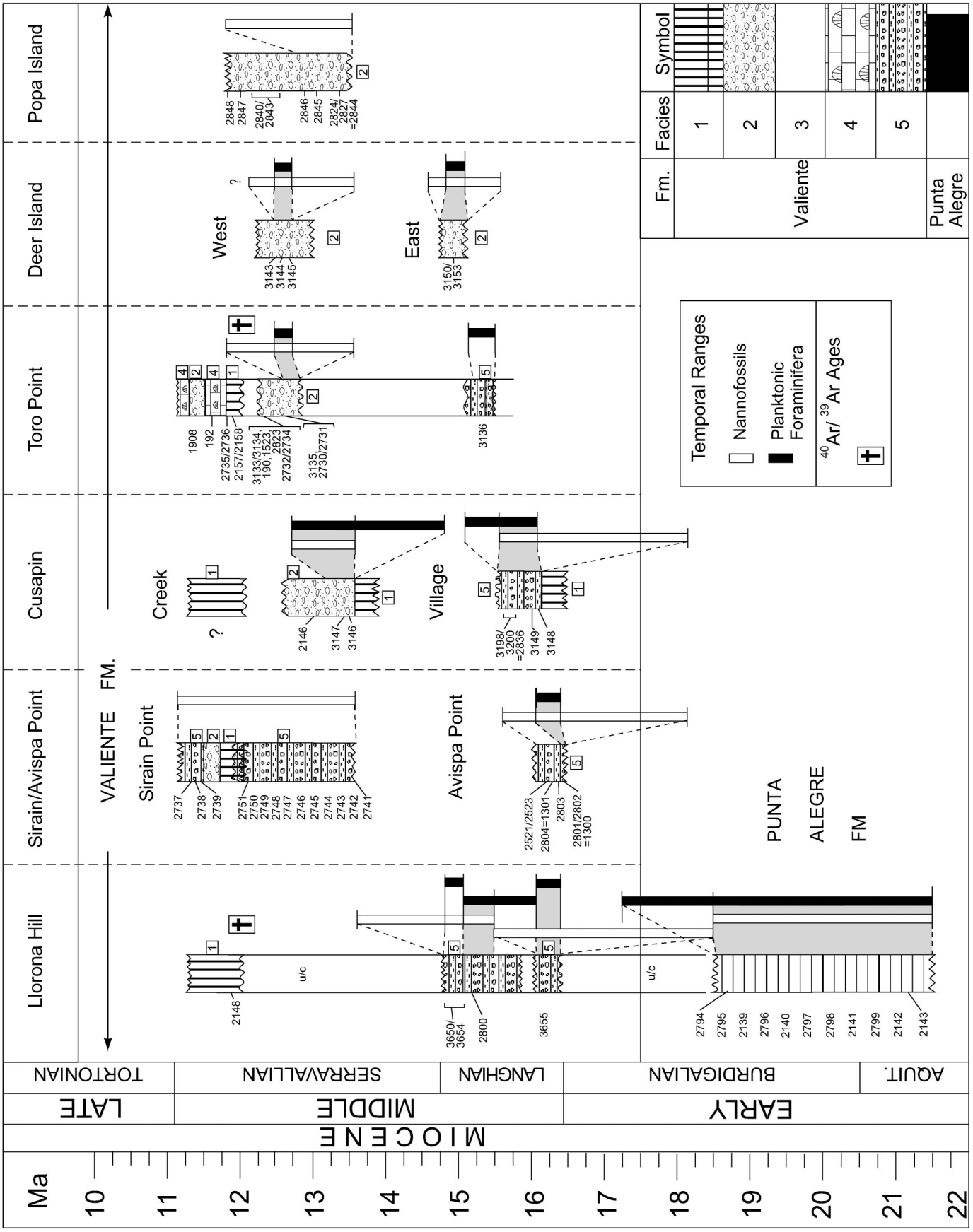
Ma
MIOCENE
LATE
MIDDLE
EARLY
TORTONIAN
SERRAVALLIAN
LANGHIAN
BURDIGALIAN
AQUIT.
Llorona Hill
Sirain/Avispa Point
Cusapin
Toro Point
Deer Island
Popa Island
VALIENTE FM.
PUNTA ALEGRE FM
Sirain Point
Avispa Point
Creek
Village
West
East
u/c
Fm.
Facies
Symbol
Valiente
Punta Alegre
Temporal Ranges
Nannofossils
Planktonic Foraminifera
40Ar/39Ar Ages

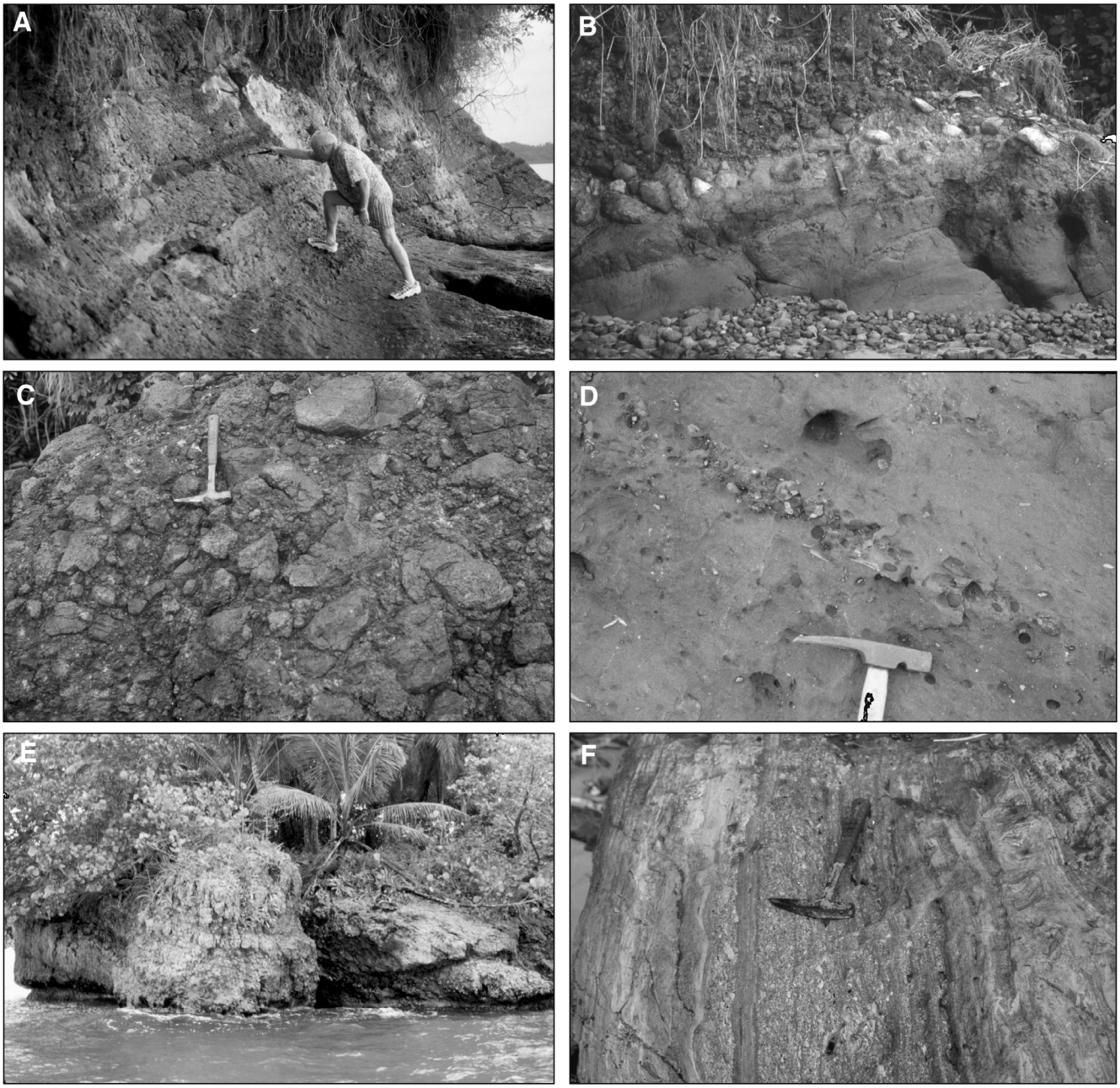


**Figure 4. Photographs of exposures of the Punta Alegre Formation and various lithofacies of the Valiente Formation. (A) Stratotype of the Punta Alegre Formation on the Valiente Peninsula, 1 km south of Bluefield Point, Valiente Peninsula, Bocas del Toro. Possible bentonite appears as a dark horizon above the hammer. (B) Slightly angular unconformable contact of the upper surface of the Punta Alegre Formation and a flow breccia of the Valiente Formation, 1 km south of Bluefield Point, Valiente Peninsula, Bocas del Toro. (C) Typical basaltic flow breccia in the stratotype of the Valiente Formation, along the coast, 900 m south of Toro Point, Valiente Peninsula, Bocas del Toro. (D) Coarse-grained volcaniclastic facies in the stratotype of the Valiente Formation, along the coast ~850 m south of Toro Point, Valiente Peninsula, Bocas del Toro. (E) Bedded reef-rubble limestone in the stratotype of the Valiente Formation at Toro Point, Valiente Peninsula, Bocas del Toro. (F) Overturned block of the turbidite lithofacies of the Valiente Formation, 1 km south of Toro Point, Valiente Peninsula, Bocas del Toro. In the photographs with a hammer for scale, the hammer head is 14 cm long and the handle is 34 cm long.**

NN6), together with *C. miopelagicus*, *D. exilis*, and *C. mexicanus*, allow confident assignment of this level to Zone NN6 (ca. 13.6–11.8 Ma). The presence of the planktic foraminifera *Globorotalia praefohsi* and *G. fohsi fohsi* at sites PPP2730–PPP2731 further restricts the age of this level to Zone N11 (= M8; ca. 12.7–12.5 Ma). The lowest site (PPP3136) in the section, located 3 m below site PPP2730, contains a planktic foraminiferal fauna that includes *P. circularis*, *P. glomerosa*, *G. venezuelana*, and *Globigerinella praesiphonifera* and clearly indicates Zone N8/M5b (ca. 15.5–15.2 Ma).

Two sections were measured along the coast of Deer Island (Figs. 2, 3). The section along the eastern coast of Deer Island is older. Sites PPP3150 and PPP3153 contain *S. heteromorphus* and *Discoaster formosus*, which indicate that the upper part of the eastern section belongs to the lower part of Zone NN5 (note that the range of *D. formosus* has not been calibrated to the geomagnetic polarity time scale [GPTS] of Cande and Kent, 1992, 1995). The planktic foraminifera at site PPP3150 include *Orbulina suturalis* and *P. circularis*, which define the age to (basal) Zone N9 (= basal Zone M6; ca. 15 Ma). The section on the northwestern coast of Deer Island (Fig. 3) is younger. The calcareous nannofossil assemblages are scarce and poorly preserved, but *S. heteromorphus* was not encountered, indicating an age younger than Zone NN5. The planktic foraminifera include *Paragloborotalia mayeri*, *G. praefohsi*, and *G.* cf. *peripheroacuta*, suggesting Zone N11.

A section in the Valiente Formation was also measured along the southeastern coast of Popa Island, immediately north of Laurel Point (Figs. 2, 3). Stratigraphic relationships are complicated in this section by the intrusion of a basalt dike ($^{40}Ar/^{39}Ar$ dates of 8.46 ± 0.04 and 8.52 ± 0.06 Ma), which locally brings some of the coarse-grained volcanic conglomerate units to vertical dips. Preservation of microfossils is poor, but they are abundant at many levels. Sites PPP2845–PPP2846 yielded *R. floridana*, *R. pseudoumbilicus*, *C. miopelagicus*, *Sphenolithus neoabies*, *Helicosphaera carteri*, *D. deflandrei*, *D. variabilis*, and *D. musicus*, which indicate an age younger than Zone NN5 (ca. 13.6 Ma). Site PPP2845 also yielded planktic foraminifera *G. trilobus*, *G. altispira*, *G. venezuelana*, *G. bisphaerica*, *Paragloborotalia mayeri*, *P. bella*, and *G. peripheroronda* (but no true orbulinids), seemingly indicative of Zone N8/M5 (ca. 16.4–15.1 Ma). *Sphenolithus heteromorphus* (indicative of Zones NN4–NN5) would have been expected if the older Zone N8 assignment were correct, but no specimens were found at sites PPP2824–PPP2827 or PPP2844–PPP2846, and we prefer the younger nannofossil age determination.

## GEOCHRONOLOGY

We dated samples of unaltered plagioclase phenocrysts (Fig. 5, Table 3) from a basalt flow from the Llorona Hill section (site PPP2148), a basalt flow from the Toro Point section (Fig. 3, PPP2157 and PPP2158), and a large dike that intrudes the Valiente Formation and extends along and just inland of the south coast of Popa Island (Fig. 3). Samples of the dike (Fig. 2) were taken at Punta Laurel (PPP2160) and ~2 km to the west (PPP2161). Analysis of the groundmass of these samples produced very disturbed $^{40}Ar/^{39}Ar$ age spectra that were not interpretable, and thus data from the basalt age spectra are not included in the following discussion. Standard methods of mineral separation, including crushing, pulverizing, magnetic separation, heavy liquids, and handpicking were used to separate >99.9% splits of plagioclase for analysis.

The age spectrum for site PPP2148 in the Llorona Hill section (Fig. 5) yielded a plateau age of 11.98 ± 0.07 Ma that includes 63.2% of the $^{39}Ar$ released in the 1100 °C through the 1300 °C steps. The apparent K/Ca ratio of the first step in the analysis (0.34) is significantly higher than the ratios of the rest of the analyses, which range from 0.08 to 0.09. Inverse isotope-correlation analysis of the age-spectrum data, including all of the data, results in an age of 12.0 ± 0.6 Ma with an initial $^{40}Ar/^{36}Ar$ ratio that is indistinguishable from that of the modern atmosphere. The good agreement of the correlation age with the plateau gives a high degree of confidence in the results.

The $^{40}Ar/^{39}Ar$ age spectrum for site PPP2157 in the Toro Point section (Fig. 5) yielded a plateau age of 11.88 ± 0.07 Ma that included 99.6% of the $^{39}Ar$ released in all but the first step of the analysis. Apparent K/Ca ratios of all of the steps in the age spectrum range from 0.06 to 0.07, indicating a high-purity plagioclase separate. Inverse isotope-correlation analysis of the age-spectrum data, excluding the first step, results in an age of 11.9 ± 0.3 Ma with an initial $^{40}Ar/^{36}Ar$ ratio that is indistinguishable from that of the modern atmosphere. The good agreement of the correlation age with the plateau gives us a high degree of confidence in the results.

The age spectrum for sample PPP2158 (Fig. 5), from the same flow as PPP2157, yielded a plateau age of 12.08 ± 0.07 Ma that includes 99.3% of the $^{39}Ar$ released in all but the first step of the analysis. Apparent K/Ca ratios range from 0.09 to 0.07 on the plateau age steps. The K/Ca ratio of the first step in the age spectrum is much lower (0.01) than the ratios on the plateau and suggests the presence of a small amount of some other phase in the sample. Inverse isotope-correlation analysis of the age-spectrum data, excluding the first step, results in an age of 12.1 ± 0.5 Ma with an initial $^{40}Ar/^{36}Ar$ ratio that is indistinguishable from that of the modern atmosphere. The good agreement of the correlation age with the plateau age gives us a high degree of confidence in the results. There is also a remarkable agreement between the estimated age of this flow (ca. 12 Ma) and Zone N11 (= M8; 12.7–12.5 Ma; Berggren et al., 1995) assigned to sites PPP2730 and PPP2731, which lie ~15 m stratigraphically lower.

The average age for the Toro Point basalt based on plagioclase samples from PPP2157 and PPP2158 is 11.98 ± 0.14 Ma (1σ). This age is indistinguishable from our age of 11.98 ± 0.06 Ma for the Llorona Hill plagioclase. The $^{40}Ar/^{39}Ar$ dates and similar K/Ca values from all three samples suggest that the same basalt flow is most likely represented in both outcrops.

The age spectra of plagioclase samples from sites PPP2060 and PPP2061 (Fig. 5), which are from the dike that intrudes the Valiente Formation, are very similar. Both have slightly U-shaped spectra suggesting the presence of excess argon. Nonetheless, the samples develop age plateaus of 8.42 ± 0.05 and 8.50 ± 0.05 Ma, respectively. The minimum ages in both age spectra agree, within the limits of analytical precision, with their respective plateau ages. Inverse isotope-correlation analysis of the gas from these samples produces apparent ages of 8.4 ± 0.4 Ma and 8.5 ± 0.5 Ma, respectively, with initial $^{40}Ar/^{36}Ar$ ratios that are atmospheric within the limits of analytical precision. Our best estimate for the age of this dike is the average of the two plateau ages, 8.46 ± 0.05 Ma (1σ).

## PALEOBATHYMETRY

Figure 6 shows the paleobathymetry of Valiente Peninsula and Popa Island determined from 27 samples examined by this study, combined with data from previous studies of the Bocas del Toro, Limón, and Panama Canal Basins (summarized by Collins et al., 1999). Paleobathymetry was inferred for each sample from the combined ecologic ranges of the benthic foraminifera, based on their known paleo-

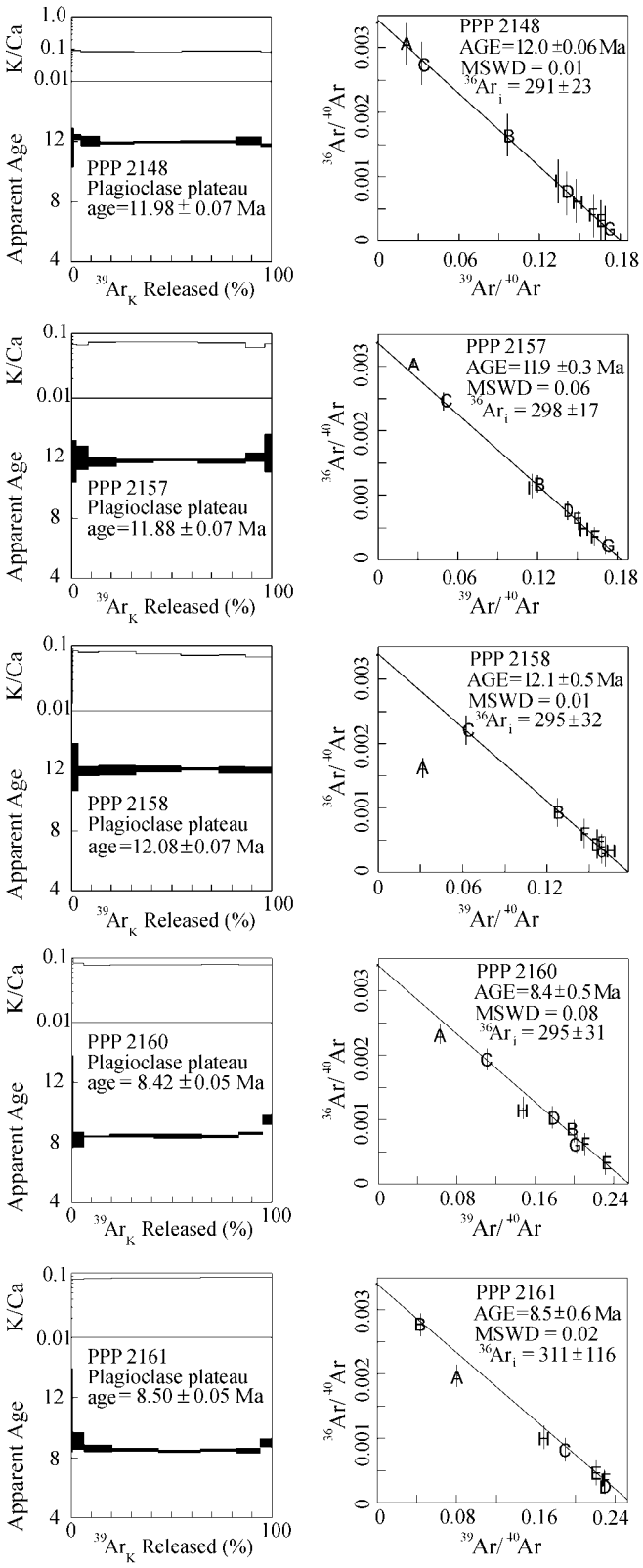


**Figure 5. $^{40}Ar/^{39}Ar$ age spectra and inverse isotope-correlation diagrams for the sites analyzed in this study. Boxes for individual analyses in age spectra are plotted at 2σ. The MSWD (mean square of weighted deviates) in the inverse isotope-correlation diagrams are goodness-of-fit indicators, and boxed points in these diagrams indicate analyses not used in the correlation.**

bathymetric distribution (e.g., Phleger and Parker, 1951; Pflum and Frerichs, 1976; van Morkhoven et al., 1986; Boersma, 1984).

The benthic foraminiferal assemblages (listed in Table 2) are generally diverse and well preserved. The taxa are especially characteristic of the Miocene southern Caribbean deposits of Panama, Costa Rica, and Venezuela (Renz, 1948; Blow, 1959). Typical deepest-dwelling taxa (and their preferred water depths) of the Punta Alegre Formation (PPP2796) include *Melonis sphaeroides* (lower bathyal–abyssal), *Uvigerina rugosa* (lower upper bathyal–middle bathyal), and *Rectuvigerina multicostata* (bathyal).

The deepest-dwelling taxa from the Valiente Formation occur in the upper Llorona Hill (PPP2800) and Deer Island (PPP3151) sections, which are middle bathyal. Taxa include *Cibicides wuellerstorfi* (middle bathyal–lower bathyal), *Melonis pompilioides* (upper bathyal–middle bathyal), *Siphonina tenuicarinata* (outer neritic–middle bathyal), and *Laticarinina pauperata* (bathyal-abyssal). There are also many upper-bathyal sections in the Valiente Formation, including Avispa Point (PPP2803), Cusapin Village (PPP3148, PPP2836), Cusapin Creek (PPP3146), Toro Point (PPP2730, 2731), and southern Popa Island (PPP2825, PPP2827, PPP2844, PPP2845, PPP2846). Taxa include the following deepest-dwelling species that are mostly upper bathyal: *Cibicidoides crebbsi*, *C. compressus*, *Bulimina mexicana*, *Uvigerina mexicana*, *Siphogenerina transversa*, and *Planulina subtenuissima*.

Taxa characteristic of the Bocas del Toro Group (upper Miocene–lower Pliocene formations, PPP2839, PPP2828, PPP2850, PPP2852, PPP2853), which are mostly middle- to outer-neritic deposits, are neritic *Elphidium* spp., *Hanzawaia concentrica*, *Trifarina eximia*, and *Reussella atlantica*; middle-neritic *Neoeponides antillarum*; outer-neritic to bathyal *Cassidulina laevigata*, *Hanzawaia isidroensa*, *Gyroidina regularis*, and *Siphogenerina lamellata*; and outer-neritic to bathyal *Hoeglundina elegans*.

The paleobathymetric history of the newly studied sections of the Punta Alegre Formation and the Valiente Formation in the Valiente Peninsula and Popa Island agree with and supplement those of the Limón and Panama Canal basins (Fig. 6). From Burdigalian to Langhian time, lower-bathyal depths (Punta Alegre Formation) in the Bocas del Toro Basin shallowed to middle-bathyal depths (Valiente Formation), and middle-bathyal water depths of the Limón Basin shallowed to upper-bathyal depths (Uscari Formation).

TABLE 3. ANALYTICAL DATA FOR SAMPLES ANALYZED IN THIS STUDY

| Temp (°C) | %$^{39}Ar_K$ of total | % radiogenic | %$^{39}Ar_K$† | $^{40}Ar^*/^{39}Ar_K$ | Apparent K/Ca | Apparent age and precision (Ma)‡ |
|---|---|---|---|---|---|---|
| #2148 | J = 0.001205 ± 0.50% | | | Plagioclase | | Sample wt 0.2140 g |
| 600 | 0.2 | 9.6 | 0.009 | 4.523 | 0.34 | 9.81 ± 9.60 |
| 700 | 1.1 | 51.4 | 0.056 | 5.345 | 0.10 | 11.59 ± 0.64 |
| 800 | 3.6 | 18.5 | 0.186 | 5.672 | 0.09 | 12.29 ± 0.09 |
| 900 | 9.3 | 78.0 | 0.484 | 5.562 | 0.08 | 12.05 ± 0.16 |
| 1000 | 17.3 | 90.9 | 0.896 | 5.492 | 0.08 | 11.90 ± 0.03 |
| 1100 | 23.6 | 88.3 | 1.227 | 5.520 | 0.08 | 11.96 ± 0.02 |
| 1200 | 27.4 | 93.6 | 1.424 | 5.539 | 0.09 | 12.00 ± 0.03 |
| 1300 | 12.2 | 81.6 | 0.631 | 5.557 | 0.09 | 12.04 ± 0.13 |
| 1400 | 5.4 | 72.6 | 0.279 | 5.422 | 0.08 | 11.75 ± 0.05 |
| Total gas | 100.0 | 84.5 | 5.193 | 5.525 | 0.09 | 11.97 |
| 63.2% of gas on plateau in 100 °C through 13000 °C steps Plateau age = 11.98 ± 0.07 | | | | | | |
| #2157 | J = 0.001207 ± 0.50% | | | Plagioclase | | Sample wt. 0.2494 g |
| 600 | 0.4 | 9.7 | 0.018 | 3.621 | 0.06 | 7.88 ± 1.00 |
| 700 | 2.1 | 65.1 | 0.101 | 5.438 | 0.07 | 11.80 ± 0.69 |
| 800 | 6.1 | 27.4 | 0.296 | 5.553 | 0.07 | 12.05 ± 0.39 |
| 900 | 13.9 | 77.4 | 0.680 | 5.424 | 0.07 | 11.77 ± 0.14 |
| 1000 | 18.2 | 82.0 | 0.890 | 5.455 | 0.07 | 11.84 ± 0.07 |
| 1100 | 22.4 | 89.3 | 1.094 | 5.485 | 0.07 | 11.90 ± 0.03 |
| 1200 | 23.7 | 93.3 | 1.159 | 5.447 | 0.07 | 11.82 ± 0.07 |
| 1300 | 9.8 | 84.9 | 0.480 | 5.563 | 0.06 | 12.07 ± 0.14 |
| 1400 | 3.4 | 65.9 | 0.167 | 5.686 | 0.07 | 12.34 ± 0.63 |
| Total gas | 100.0 | 81.5 | 0.000 | 5.473 | 0.07 | 11.88 |
| 99.6% of gas on plateau in 700 °C through 14000 °C steps Plateau age = 11.88 ± 0.07 | | | | | | |
| #2158 | J = 0. 001195 ± 0.50% | | | Plagioclase | | Sample wt. 0.2502 g |
| 600 | 0.7 | 51.9 | 0.029 | 16.321 | 0.01 | 34.85 ± 3.08 |
| 700 | 2.9 | 72.5 | 0.126 | 5.688 | 0.09 | 12.22 ± 0.79 |
| 800 | 10.1 | 34.7 | 0.443 | 5.564 | 0.08 | 11.96 ± 0.14 |
| 900 | 18.5 | 87.0 | 0.810 | 5.594 | 0.08 | 12.02 ± 0.15 |
| 1000 | 22.4 | 89.5 | 0.985 | 5.626 | 0.08 | 12.09 ± 0.10 |
| 1100 | 19.1 | 82.3 | 0.838 | 5.629 | 0.07 | 12.10 ± 0.04 |
| 1150 | 13.2 | 89.2 | 0.581 | 5.608 | 0.07 | 12.05 ± 0.10 |
| 1200 | 13.2 | 90.5 | 0.578 | 5.591 | 0.07 | 12.02 ± 0.11 |
| Total gas | 100.0 | 81.5 | 0.000 | 5.681 | 0.08 | 12.21 |
| 99.3% of gas on plateau in 700 °C through 1200 °C steps Plateau age = 12.08 ± 0.07 | | | | | | |
| #2160 | J = 0.001250 ± 0.50% | | | Plagioclase | | Sample wt. = 0.2501 g |
| 600 | 0.9 | 31.2 | 0.053 | 4.935 | 0.10 | 110.70 ± 1.53 |
| 700 | 5.1 | 75.8 | 0.289 | 3.786 | 0.08 | 8.22 ± 0.25 |
| 800 | 13.0 | 43.0 | 0.736 | 3.879 | 0.08 | 8.42 ± 0.02 |
| 900 | 22.2 | 69.4 | 1.257 | 3.908 | 0.08 | 8.48 ± 0.05 |
| 1000 | 23.9 | 90.5 | 1.356 | 3.891 | 0.08 | 8.44 ± 0.07 |
| 1100 | 18.5 | 81.8 | 1.047 | 3.877 | 0.08 | 8.41 ± 0.03 |
| 1200 | 11.7 | 80.7 | 0.662 | 3.980 | 0.08 | 8.64 ± 0.05 |
| 1300 | 4.8 | 65.2 | 0.270 | 4.403 | 0.08 | 9.55 ± 0.16 |
| Total gas | 100.0 | 74.4 | 0.000 | 3.930 | 0.08 | 8.53 |
| 83.6% of gas on plateau in 600 °C through 1100 °C steps Plateau age = 8.42 ± 0.05 | | | | | | |
| #2161 | J = 0.001204 ± 0.50% | | | Plagioclase | | Sample wt. = 0.2495 |
| 700 | 0.7 | 41.7 | 0.041 | 5.151 | 0.08 | 11.16 ± 1.38 |
| 800 | 5.7 | 18.4 | 0.330 | 4.203 | 0.08 | 9.11 ± 0.28 |
| 900 | 13.6 | 75.5 | 0.783 | 3.980 | 0.08 | 8.63 ± 0.12 |
| 1000 | 23.2 | 90.6 | 1.333 | 3.946 | 0.09 | 8.55 ± 0.05 |
| 1100 | 21.3 | 86.0 | 1.225 | 3.893 | 0.08 | 8.44 ± 0.04 |
| 1200 | 18.0 | 90.1 | 1.034 | 3.935 | 0.09 | 8.53 ± 0.04 |
| 1300 | 11.7 | 86.5 | 0.670 | 3.911 | 0.09 | 8.48 ± 0.08 |
| 1400 | 5.8 | 69.9 | 0.332 | 4.153 | 0.09 | 9.00 ± 0.14 |
| Total gas | 100.0 | 81.3 | 0.000 | 3.969 | 0.09 | 8.60 |
| 87.8% of gas on plateau in 9000 °C through 13000 °C steps Plateau age = 8.50 ± 0.05 | | | | | | |

*Notes*: $^{40}Ar/^{39}Ar$ analyses were conducted using a MAP 215 rare gas mass spectrometer. About 0.25 mg of plagioclase from each of our samples was irradiated in the core of the U.S. Geological Survey TRIGA reactor (Dalrymple et al., 1981) to convert a portion of the 39K in the sample to$^{39}Ar$. FCT-3 sanidine was irradiated along with the samples to monitor this conversion (McDougall and Harrison, 1988). An age of 27.79+ 0.07 Ma was used for FCT-3 sanidine (Kunk et al., 1985). The irradiated plagioclase samples were heated in a low blank furnace similar in design to that of Staudacher et al. (1978) and were degassed in a stepwise manner to produce an age spectrum. Individual increments of gas were cleaned using SAES ST 707 and ST101 getters, and a Ti getter prior to analysis in the MAP 215 mass spectrometer. The resultant argon isotopic data were reduced and analytical errors calculated with an updated version of the computer program ArAr*(Haugerud and Kunk, 1988), using the decay constant values recommended by Steiger and Jäeger (1977). Corrections used for the production of interfering isotopes during irradiation are those of Dalrymple et al. (1981) and Roddick (1983). All uncertainties are stated at 1ó. The occurrence of age plateau was determined using the definition of Fleck et al. (1977) as modified by Haugerud and Kunk (1988). A rigorous discussion of the error propagation calculations, as well as age calculations, can be found in Haugerud and Kunk (1988). The$^{40}Ar/^{39}Ar$ age spectrum data for all of the samples can be found in Table 3 and Figure 4.

†$^{39}Ar_K$ gas quantities are in moles × $10^{-1}$.

‡All precision estimates are at the one sigma level. Ages of individual steps do not include error in the irradiation parameter J. No error is calculated for the total gas age. The plateau age includes the error in the irradiation parameter J. Ages calculated assuming an initial$^{40}Ar/^{36}Ar$ = 295.5 ± 0.

From the Langhian to middle Serravallian time there was no discernible bathymetric change in either the Bocas del Toro or Limón basins (Fig. 6). In late Serravallian time (ca. 12 Ma), upper bathyal deposition (Valiente Formation) in the Bocas del Toro Basin changed to alternating deposition of terrestrial and nearshore sedimentary rocks, as indicated by coarse-grained basaltic flow breccia and coral-reef limestone with large colonies of hermatypic corals that crop out in the Toro Point section. Upper Serravallian to middle Tortonian deposits of the Panama Canal Basin (Gatun Formation) also reflect inner- to middle-neritic depths (Collins et al., 1996). Shallow depths persisted in the Bocas del Toro Basin until late Tortonian to Messinian time, as indicated by the Tobabe Sandstone, coarse-grained nearshore marine conglomeratic sandstone packed with large sand dollars and large bivalves. Later in the Messinian, the depths decreased to upper bathyal, represented by the Nancy Point Formation. By Zanclean time, water depths had shallowed from upper bathyal to neritic in both the Bocas del Toro Basin (Shark Hole Point and Cayo Agua Formations) and the Limón Basin (Rio Banano, Quebrada Chocolate, and Moin Formations).

## DISCUSSION

The discovery of the Punta Alegre Formation and Valiente Formation extends the geologic history of the Bocas del Toro Basin from ca. 8 Ma (the base of the Bocas del Toro Group; Coates et al., 1992; Coates, 1999) back to early Miocene time, ca. 18–21 Ma. The lower-bathyal (1000–2000 m), muddy and silty ooze of the Punta Alegre Formation records the pre-isthmian tropical American ocean. Coeval deposits, like the Uscari Formation in the southern Limón Basin (Cassell and Sen Gupta, 1989b; Bottazzi et al., 1994) and the Clarita and Tapaliza Formations of the Darien region (Collins et al., 1998), were also deposited at bathyal depths. This finding suggests that an extensive oceanic gap existed between the Central American volcanic arc and South America.

Evidence from the overlying Valiente Formation indicates the rapid rise of the pre-isthmian sill between 18 and 16 Ma (Figs. 6, 7A). Middle Miocene (Langhian; 16.4–14.8 Ma) deposits at Avispa Point, Toro Point, and Cusapin Village indicate upper-bathyal (200–600 m) paleodepths, and those at Llorona Hill and Deer Island record middle-bathyal (600–1000 m) paleodepths. These turbidite and resedimented shelly units presumably formed on the unstable slope of the rising isthmian arc.

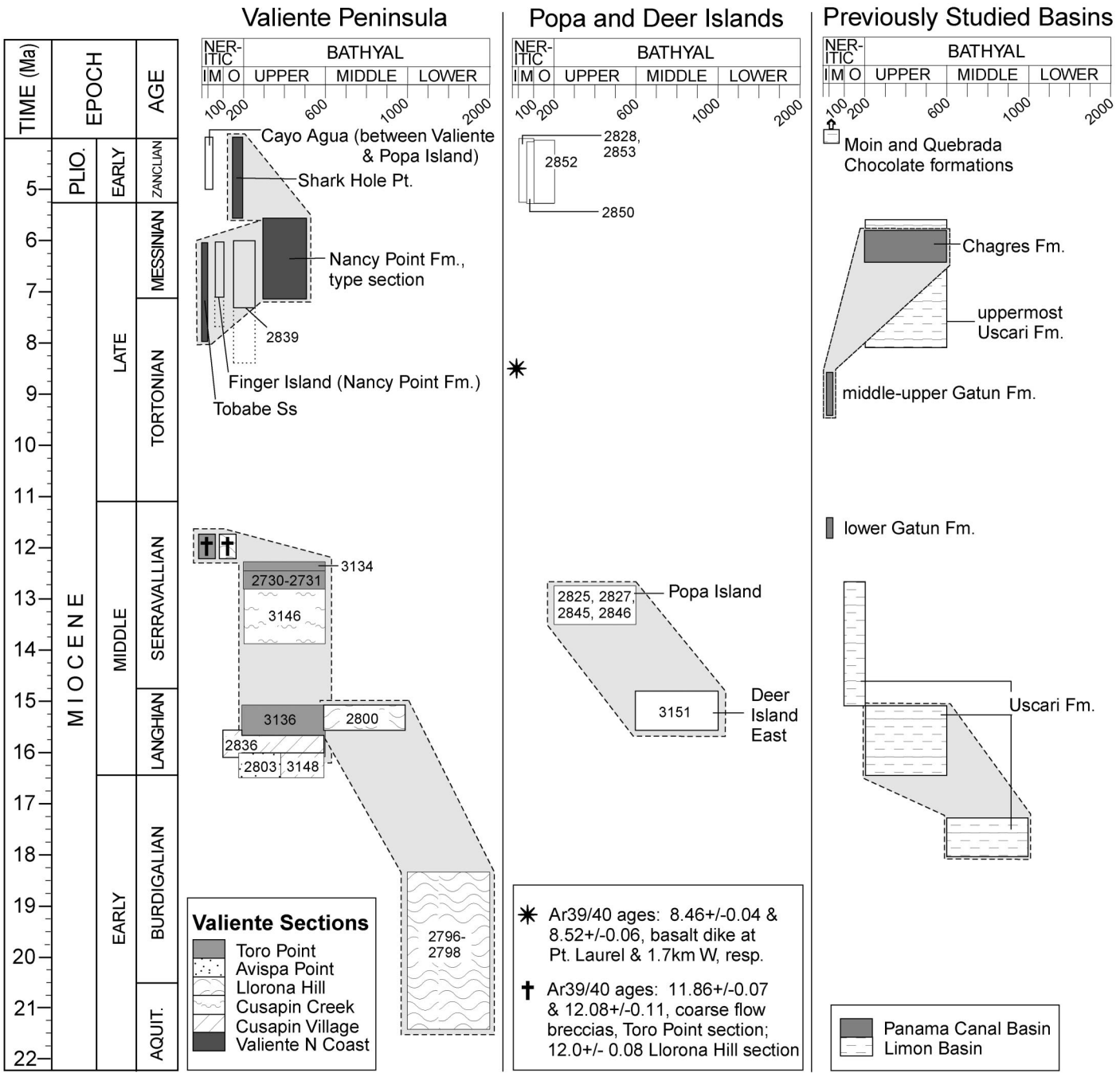


**Figure 6. Chronological chart showing bathymetric ranges of PPP sites (numbered) determined by benthic foraminifera for various ages from the Valiente Peninsula, Popa Island, and the southern Limón and Panama Canal basins. Dashed lines enclose the same geologic section. Dotted lines show the biochronologic ranges of sections that are placed according to physical stratigraphy.**

A similar bathymetric sequence is recorded for the Uscari Formation in the southern Limón Basin.

Middle- and upper-bathyal paleodepths were sustained through the lower part of the Serravallian in the upper Toro Point and Cusapin Creek sections (Fig. 6). Further rapid shallowing in late Serravallian time is, however, signaled by the widespread development of columnar basalt lava; flow breccia; fluviatile to estuarine, coarse-grained volcaniclastic deposits; lahars; and intercalated reef lenses packed with large coral heads. These rocks testify to the extensive emergence of the isthmian volcanic arc in the Bocas del Toro area by 12 Ma (Fig. 7B).

The reef lenses in the Valiente Formation appear to represent patchy shallow-water fringing reefs around volcanic islands whose flanks were otherwise characterized by laharic breccia and basalt flows. The lahars and flows grade laterally into fluviatile and deltaic sequences and nearshore marine deposits. Volcanic activity in the area appears to have

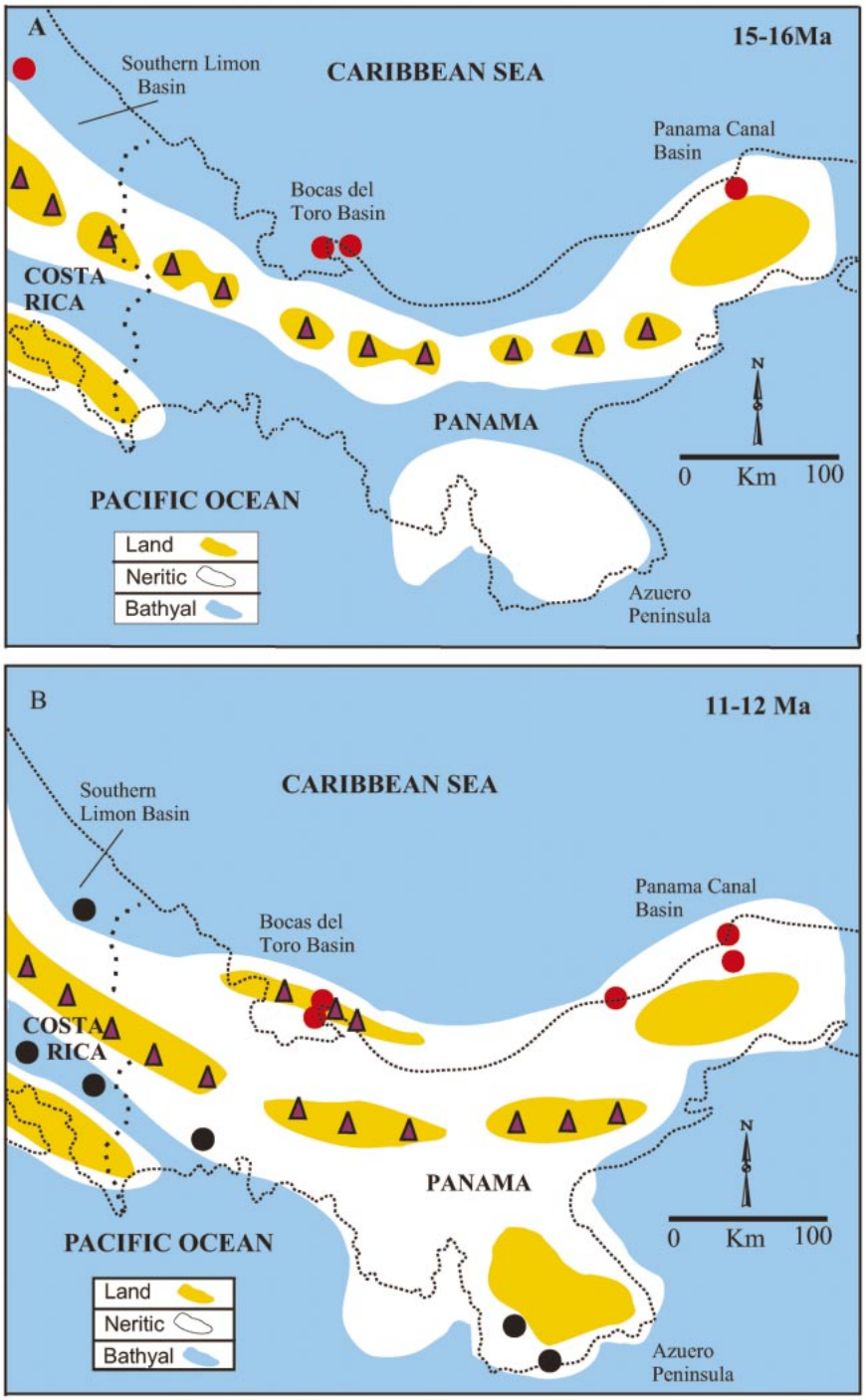


**Figure 7. (A) Schematic paleogeographic reconstruction of the Isthmus of Panama at 15–16 Ma. Circles represent reliably dated sections that have yielded rich benthic foraminiferal assemblages useful for paleobathymetric analysis. The Central Cordilleran volcanic arc is shown as a line of islands; the triangles represent volcanoes. Evidence of middle Miocene volcanism in western Panama is from de Boer et al. (1988, 1991) and references therein. Land areas to the south of the arc are interpreted as exotic terranes. The Panamanian Isthmus at this stage was a volcanic island arc with a narrow neritic zone. The sedimentary rocks of the Southern Limón and Bocas del Toro Basins indicate bathyal paleodepths in contrast to the Panama Canal Basin, where neritic to emergent conditions persisted through most of the Cenozoic. (B) Schematic paleogeographic reconstruction of the Isthmus of Panama at 11–12 Ma. Symbols as for A. The neritic zone has by this time expanded significantly, and an emergent active volcanic backarc has developed in the Bocas del Toro Basin. We assume that the Central Cordilleran volcanic arc has become more emergent.**

ceased by ca. 8 Ma. Two $^{40}Ar/^{39}Ar$ samples from a basalt dike in the Valiente Formation exposed at Laurel Point on Popa Island yield ages of 8.46 ± 0.04 Ma and 8.52 ± 0.06 Ma, respectively (Fig. 6). The youngest igneous volcanic rocks recorded in the Bocas del Toro area are from the basalt dike exposed at Laurel Point in Popa Island dated at ca. 8.5 Ma.

Coeval (ca. 11.8–11.4 Ma) inner neritic deposits in the Panama Canal Basin (Collins et al., 1996) suggest that the emergence of the isthmus had simultaneously developed to a similar degree in the Panama Canal Basin (Fig. 7B). To the northwest, in the southern Limón Basin, shallowing was slower because there the uppermost Uscari Formation records upper-bathyal (200–600 m) paleodepths (Fig. 7B) as late as the latest Miocene (Messinian, 7.26–5.32 Ma). Middle Miocene deposits (Langhian and Serravallian; ca. 16.4–11.2 Ma) in the Darien region (Clarita and Tapaliza Formations; Collins et al., 1998), and Burdigalian through Messinian sedimentary rocks (ca. 20–6 Ma) of the Atrato Basin in the Pacific coastal region of northwest Colombia (Uva, Napipi, and Sierra Formations; Duque-Caro, 1990), also record continuing bathyal paleodepths until the latest Miocene (Fig. 6). This fact suggests that a deep-water gap still existed between the Central American volcanic arc and South America at this time, presumably responsible for the virtual absence of exchange of terrestrial vertebrate faunas between North and South America until middle Pliocene time (2.8 Ma).

In the Bocas del Toro Basin, the Valiente Formation is unconformably overlain by the Tobabe Sandstone Formation (Coates et al., 1992; Coates, 1999), indicating continued very shallow, marginal marine conditions. Sedimentary rocks of the conformably overlying Nancy Point Formation (Messinian, 7.26–5.32 Ma; Aubry and Berggren, 1999) show that deepening proceeded to upper-bathyal depths (200–600 m; Collins, 1993) in the Messinian. This deepening is also recorded in the Panama Canal Basin (Fig. 6) by the

rapid transition from the inner neritic (20–40 m), middle to upper Gatun Formation to the upper bathyal Chagres Formation (Collins et al., 1996). It is not clear whether this deepening represents a regional eustatic event or local cooling and sinking of the Bocas del Toro volcanic arc. By the early Pliocene (Zanclean), rapid shallowing again occurred in the Bocas del Toro Basin (Shark Hole Point and Cayo Agua Formations, Fig. 6) as in the southern Limón Basin of Costa Rica (Fig. 4, Limón Group; McNeill et al., 1999).

## CONCLUSIONS

The Punta Alegre Formation and the Valiente Formation document the earliest stages of the rise of the Isthmus of Panama in the Bocas del Toro region. Evidence of the pre-isthmian tropical American ocean is provided by the Punta Alegre Formation, which ranges in age from ca. 18.5 to 21.5 Ma, and accumulated in lower bathyal water depths. Coeval deposits with similar paleobathymetry, like the Uscari Formation in the southern Limón Basin of Costa Rica and the Uva and Napipi Formations of the Atrato Basin in northwest Colombia, confirm the presence of this widespread ocean separating North and South America.

The distribution of the Valiente Formation facies suggests that, around the Bocas del Toro Basin, the pre-isthmian sill rose to middle bathyal (Llorona Hill and Deer Island sections) and upper bathyal (Avispa and Toro Points and Cusapin Village sections) paleodepths between ca. 18 and 15 Ma and lay to the north of a sparsely emergent Central Cordilleran arc (Fig. 7A). These paleodepths persisted until early Serravallian time (ca. 15–13 Ma). In the late Serravallian, the pre-isthmian sill in the Bocas del Toro region shallowed rapidly, so that by ca. 12 Ma there was an active, emergent volcanic backarc (Fig. 7B) parallel to the main Central Cordilleran arc.

Coeval sedimentary rocks deposited in shallow water also occur in the Panama Canal Basin (Gatun Formation), but shallowing was slower in the southern Limón Basin where the upper Uscari Formation indicates upper bathyal (200–600 m) paleodepths (Fig. 7B). Bathyal depths also prevailed in the Darien region of eastern Panama and in the Atrato Basin of northwestern Colombia until the latest Miocene. This fact suggests a continued albeit more narrow oceanic gap between South America and the Central American isthmus, also confirmed by the absence of any connection of terrestrial faunas of North and South America until late Pliocene time (Webb and Rancy, 1996).

In the Bocas del Toro region, inner neritic paleodepths, represented by the Tobabe Sandstone, prevailed until the Messinian (7.26–5.32 Ma), when widespread deepening to upper bathyal depths is recorded by the overlying Nancy Point Formation. This event was paralleled in the Panama Canal Basin by the transition from the Gatun Formation (ca. 8 Ma, 20–40 m paleodepth) to the overlying Chagres Formation (ca. 6 Ma, 200–600 m paleodepth). In the Bocas del Toro region, depths subsequently shallowed to inner neritic depths (Shark Hole Point and Cayo Agua Formations; 5.2–3.5 Ma). Coeval deposits in the southern Limón Basin (Rio Banano, Quebrada Chocolate, Moin, and Suretka Formations) also record rapid shallowing and emergence in this region. The cause of the Messinian (7.26–5.32 Ma) deepening event in the Bocas del Toro and Panama Canal basins is not clear. Cooling and sinking of the Bocas del Toro volcanic arc, after ca. 8 Ma, is not easily extrapolated to the Panama Canal Basin. However, more detailed work in the southern Limón Basin and the Darien region is necessary before a eustatic cause can be unequivocally established.

## ACKNOWLEDGMENTS

We are deeply grateful to Xenia Saavedra de Guerra for editing the manuscript, producing Figures 1, 2, and 3, and compiling the occurrence charts of nannofossils and planktic foraminifera (Table 1). We are also grateful to Jijun Zhang and Huichan Lin for preparation of foraminiferal and nannofossil samples, respectively, and to Deanna Hurt for preparation of benthic foraminiferal samples. All microfossil samples are deposited in the Smithsonian Institution, National Museum of Natural History. Collins and Coates gratefully acknowledge grants DEB-9300905 and DEB-9696123 from the National Science Foundation. Field work and sample preparations were made possible by awards from the National Geographic Society. Coates was also supported by grants from the Scholarly Studies Program and Walcott Funds of the Smithsonian Institution. The manuscript has greatly benefited from insightful reviews by Susan Kidwell, Jelle Zeilinga de Boer, and Nancy Riggs.

## REFERENCES CITED

Aubry, M.-P., and Berggren, W.O., 1999, Appendix 1, New biostratigraphy, *in* Collins, L.S., and Coates, A.G., eds., A paleobiotic survey of Caribbean faunas from the Neogene of the Isthmus of Panama: Bulletins of American Paleontology, no. 357, p. 38–40.

Berggren, W.A., Kent, D.V., Swisher, C.C., III, and Aubry, M.-P., 1995, A revisited Cenozoic geochronology and chronostratigraphy, *in* Berggren, W.A., Kent, D.V., Aubry, M.-P., and Hardenbol, J., eds., Geochronology time scales and global stratigraphic correlation: SEPM (Society for Sedimentary Geology) Special Publication 54, p. 129–212.

Blow, W.H., 1959, Age, correlation, and biostratigraphy of the upper Tocuy (San Lorenz) and Pozon formations, eastern Falcon, Venezuela: Bulletins of American Paleontology, no. 39, p. 67–251.

Boersma, A., 1984, Handbook of common Tertiary Uvigerina: Stony Point, New York, Microclimates Press, p. 1–207.

Bottazzi, G., Fernandez, J.A., and Barboza, G., 1994, Sedimentologia e historia tectono-sedimentaria de la cuenca Limón Sur: Profil, v. 7, p. 351–391.

Budd, A.F., and Johnson, K.G., 1997, Coral reef community dynamics over 8 million years of evolutionary time: Stasis and turnover: Proceedings of the 8th International Coral Reef Symposium, p. 423–428.

Cande, S.C., and Kent, D.V., 1992, A new geomagnetic polarity time scale for the Late Cretaceous and Cenozoic: Journal of Geophysical Research, v. 97, p. 13,917–13,951.

Cande, S.C., and Kent, D.V., 1995, Revised calibration of the geomagnetic polarity time scale for the Late Cretaceous and Cenozoic: Journal of Geophysical Research, v. 100, p. 6093–6095.

Cassell, D.T., and Sen Gupta, B.K., 1989a, Pliocene foraminifera and environments, Limón Basin of Costa Rica: Journal of Paleontology, v. 63, p. 146–157.

Cassell, D.T., and Sen Gupta, B.K., 1989b, Foraminiferal stratigraphy and paleo-environments of the Tertiary Uscari Formation, Limón Basin, Costa Rica: Journal of Foraminiferal Research, v. 19, p. 52–71.

Coates, A.G., 1999, Lithostratigraphy of the Neogene strata of the Caribbean coast from Limón, Costa Rica to Colon, Panama, *in* Collins, L.S., and Coates, A.G., eds., A paleobiotic survey of Caribbean faunas from the Neogene of the Isthmus of Panama: Bulletins of American Paleontology, no. 357, p. 17–38.

Coates, A.G., and Obando, J.A., 1996, The geologic evolution of the Central American isthmus, *in* Jackson, J.B.C., Budd, A.F., and Coates, A.G., eds., Evolution and environment in tropical America: Chicago, University of Chicago Press, p. 21–56.

Coates, A.G., Jackson, J.B.C., Collins, L.S., Cronin, T.M., Dowsett, H.J., Bybell, L.M., Jung, P., and Obando, J., 1992, Closure of the Isthmus of Panama: The near-shore marine record of Costa Rica and western Panama: Geological Society of America Bulletin, v. 104, p. 814–828.

Collins, L.S., 1993, Neogene paleoenvironments of the Bocas del Toro Basin, Panama: Journal of Paleontology, v. 67, p. 699–710.

Collins, L.S., and Coates, A.G., 1999, eds., A paleobiotic survey of Caribbean faunas from the Neogene of the Isthmus of Panama: Bulletins of American Paleontology, no. 357, 351 p.

Collins, L.S., Coates, A.G., Jackson, J.B.C., and Obando, J., 1995, Timing and rates of emergence of the Limón and Bocas del Toro basins: Caribbean effects of Cocos Ridge subduction?: Geological Society of America Special Paper 295, p. 263–289.

Collins, L.S., Coates, A.G., Berggren, W.A., Aubry, M.-P., and Zhang, J., 1996, The late Miocene Panama isthmian strait: Geology, v. 24, p. 687–690.

Collins, L.S., Coates, A.G., Aubry, M.-P., and Berggren, W.A., 1998, The Neogene depositional history of Darien, Panama: Geological Society of America Abstracts with Programs, v. 30, no. 7, p. A26.

Collins, L.S., Aguilera, O., Borne, P.F., and Cairns, S.D., 1999, A paleoenvironmental analysis of the Neogene of Caribbean Panama and Costa Rica using several phyla, *in* Collins, L.S., and Coates, A.G., eds., A paleobiotic survey of Caribbean faunas from the Neogene of the Isthmus of Panama: Bulletins of American Paleontology, no. 357, p. 81–87.

Dalrymple, G.B., Alexander, E.C., Lanphere, M.A., and Kracker, G.P., 1981, Irradiation of samples for $^{40}Ar/^{39}Ar$ dating using the Geological Survey TRIGA reactor: U.S. Geological Survey Professional Paper 1176, 55 p.

de Boer, J.Z., Defant, M.J., Stewart, R.H., Restrepo, J.F., Clark, L.F., and Ramirez, A.H., 1988, Quaternary calc-alkaline volcanism in western Panama: Regional variation and implication for the plate tectonic frame-

work: Journal of South American Earth Sciences, v. 1, no. 3, p. 275–293.
de Boer, J.Z., Defant, M.J., Stewart, R.H., and Bellon, H., 1991, Evidence for active subduction below western Panama: Geology, v. 19, p. 649–652.
Duque-Caro, H., 1990, Neogene stratigraphy, palaeoceanography and palaeobiogeography in northwest South America and the evolution of the Panama Seaway: Palaeogeography, Palaeoclimatology, Palaeoecology, v. 77, p. 203–234.
Fleck, R.J., Sutter, J.F., and Elliot, D.H., 1977, Interpretation of discordant $^{40}Ar/^{39}Ar$ age spectra of Mesozoic tholeiites from Antarctica: Geochimica et Cosmochimica Acta, v. 41, p. 15–32.
Haugerud, R.A., and Kunk, M.J., 1988, ArAr*: A computer program for reduction of $^{40}Ar$-$^{39}Ar$ data: U.S. Geological Survey Open-File Report 88–261, 67 p.
Jackson, J.B.C., and D'Croz, L., 1999, The ocean divided, *in* Coates, A.G., ed., Central America: A natural and cultural history: New Haven, Yale University Press, p. 38–71.
Jackson, J.B.C., Jung, P., Coates, A.G., and Collins, L.S., 1993, Diversity and extinction of tropical American mollusks and emergence of the Isthmus of Panama: Science, v. 260, p. 1624–1626.
Kunk, M.J., Sutter, J.F., and Naeser, C.W., 1985, High-precision $^{40}Ar/^{39}Ar$ ages of sanidine, biotite, hornblende, and plagioclase from the Fish Canyon Tuff, San Juan volcanic field, south-central Colorado: Geological Society of America Abstracts with Programs, v. 17, p. 636.
McDougall, Ian, and Harrison, T.M., 1988, Geochronology and thermochronology by the $^{40}Ar/^{39}Ar$ method: New York, Oxford University Press, 269 p.
McNeill, D.F., Coates, A.G., Budd, A.F., and Borne, P.F., 1999, Integrated biological and paleomagnetic stratigraphy of late Neogene deposits around Limón, Costa Rica: A coastal emergence record of the Central American isthmus: Geological Society of America Bulletin, v. 112, p. 963–981.
Pflum, C.E., and Frerichs, W.E., 1976, Gulf of Mexico deep-water foraminifers: Cushman Foundation for Foraminiferal Research Special Publication 14, p. 1–125.
Phleger, F.B., and Parker, F.L., 1951, Ecology of foraminifera, northwest Gulf of Mexico. Part II: Foraminifera species: Geological Society of America Memoir 46, p. 1–64.
Renz, H.H., 1948, Stratigraphy and fauna of the Agua Salada Group, State of Falcon, Venezuela: Geological Society of America Memoir 32, 219 p.
Roddick, J.C., 1983, High precision intercalibration of $^{40}Ar/^{39}Ar$ standards: Geochimica et Cosmochimica Acta, v. 47, p. 887–898.
Staudacher, Th., Jessberger, E.K., Dorflinger, D., and Kiko, J., 1978, A refined ultrahigh-vacuum furnace for rare gas analysis: Journal of Physical Earth Science Instrumentation, v. 11, p. 781–784.
Stehli, F.G., and Webb, S.D., eds., 1985, The great American biotic interchange: New York, Plenum Press, 532 p.
Steiger, R.H., and Jaeger, E., 1977, Subcommission on geochronology—Convention on the use of decay constants in geo- and cosmochronology: Earth and Planetary Science Letters, v. 36, p. 359–362.
van Morkhoven, F.P.C.M., Berggren, W.A., and Edwards, A.S., 1986, Cenozoic cosmopolitan deepwater benthic foraminifera: Bulletin du Centre de Recherches de Pau, Memoire 11, p. 1–429.
Webb, S.D., 1999, The great American faunal interchange, *in* Coates, A.G., ed., Central America: A natural and cultural history: New Haven, Yale University Press, p. 97–122.
Webb, S.D., and Rancy, A., 1996, Late Cenozoic evolution of the neotropical mammal fauna, *in* Jackson, J.B.C., Budd, A.F., and Coates, A.G., eds., Evolution and environment in tropical America: Chicago, University of Chicago Press, p. 335–358.

MANUSCRIPT RECEIVED BY THE SOCIETY 27 MARCH 2001
REVISED MANUSCRIPT RECEIVED 13 JUNE 2002
MANUSCRIPT ACCEPTED 17 JUNE 2002

Printed in the USA